Hierarchically structured bioinspired nanocomposites

Hierarchically Structured Bioinspired Nanocomposites

Dhriti Nepal,[1] Saewon Kang,[2] Katarina M. Adstedt,[3] Krishan Kanhaiya,[4] Michael Rainer Bockstaller,[5] L. Catherine Brinson,[6] Markus J. Buehler,[7] Peter V. Coveney,[8] Kaushik Dayal,[9] Jaafar A. El-Awady,[10] Luke Christian Henderson,[11] David L. Kaplan,[12] Sinan Keten,[13] Nicholas A. Kotov,[14] George C. Schatz,[15] Silvia Vignolini,[16] Fritz Vollrath,[17] Yusu Wang,[18] Boris I. Yakobson,[19, 20] Vladimir V. Tsukruk,[21] Hendrik Heinz[22]

[1] Materials and Manufacturing Directorate, Air Force Research Laboratory, Wright-Patterson AFB, Dayton, Ohio 45433

[2] School of Materials Science and Engineering, Georgia Institute of Technology, Atlanta, GA 30332

[3] School of Materials Science and Engineering, Georgia Institute of Technology, Atlanta, GA 30332

[4] Department of Chemical and Biological Engineering, University of Colorado at Boulder, Boulder, CO 80301

[5] Department of Materials Science and Engineering, Carnegie Mellon University, Pittsburgh, PA 15213

[6] Department of Mechanical Engineering and Materials Science, Duke University, Durham, NC 27708

[7] Department of Civil and Environmental Engineering, MIT, Cambridge, MA 02139

[8] Department of Chemistry, University College London, London, WC1E 6BT, UK

[9] Department of Civil and Environmental Engineering, Carnegie Mellon University, Pittsburgh, PA 15213

[10] Department of Mechanical Engineering, Johns Hopkins University, Baltimore, MD 21218

[11] Institute for Frontier Materials, Deakin University, Waurn Ponds VIC 3216, Australia

[12] Department of Biomedical Engineering, Tufts University, Medford, MA 02155

[13] Department of Mechanical Engineering, Northwestern University, Evanston, IL 60208

[14] Department of Chemical Engineering, University of Michigan, Ann Arbor, MI 48109

[15] Department of Chemistry, Northwestern University, Evanston, IL 60208

[16] Department of Chemistry, University of Cambridge, Cambridge CB2 1EW, UK

[17] Department of Zoology, University of Oxford, Oxford OX2 8QJ, UK

[18] Halıcıoğlu Data Science Institute, University of California San Diego, La Jolla, CA 92093

[19] Department of Materials Science and Nanoengineering, Rice University, Houston, TX 77005

[20] Department of Chemistry, Rice University, Houston, TX 77005

[21] School of Materials Science and Engineering, Georgia Institute of Technology, Atlanta, GA 30332

[22] Department of Chemical and Biological Engineering, University of Colorado at Boulder, Boulder, CO 80301

Corresponding authors: Dhriti Nepal, dhriti.nepal.1@afrl.af.mil; Vladimir Tsukruk, vladimir@mse.gatech.edu; Hendrik Heinz, hendrik.heinz@colorado.edu

Abstract

Next-generation structural materials are expected to be lightweight, high strength, and tough composites with embedded functionalities to sense, adapt, self-repair, morph, and restore. This review highlights recent developments and concepts in bioinspired nanocomposites, emphasizing tailoring the architecture, interphases, and confinement to achieve dynamic and synergetic responses. We highlight cornerstone examples from natural materials with unique mechanical property combinations based on relatively simple building blocks produced in aqueous environments at ambient conditions. A particular focus is on structural hierarchies across multiple length scales to achieve multifunctionality and robustness. We further discuss recent advances, trends, and emerging opportunities in combining biological and synthetic components, state-of-the-art characterization, and modelling approaches to assess the physical principles underlying nature design and mechanical responses at multiple length scales. These multidisciplinary approaches promote the synergetic enhancement of individual materials properties and an improved predictive and prescriptive design of the next era of structural materials at multi-length scales for a wide range of applications.

1. Introduction

Nature has mastered the fabrication of hierarchical multifunctional materials, which in many ways surpass their synthetic counterparts, in an evolutionary process over millions of years.[1,2] The astonishing results have been achieved by taking advantage of diverse fundamental molecular interactions in a small set of building blocks at ambient conditions (Box 1). In particular, the evolutionary development of multi-layer hierarchical structures with unique and sometimes contradictory properties, such as combined high strength and toughness, provides great inspiration for modern materials engineering. Mimicking nature's hierarchical microstructures in synthetic composites can lead to more damage-tolerant architectures, and some bioinspired materials are already implemented in various applications.[3] The new frontiers lie in introducing sustainable, hierarchical, and dynamic composites that are multifunctional and environmentally friendly. Hereby, engineering of bioinspired structures faces many challenges, including the realization of molecular-scale precision within each level of the hierarchy, structural coupling between hard and soft building blocks, the retention of mechanical integrity while having a good balance of other functional properties, as well as the ability for fast and large-scale production.

One grand challenge to developing bio-inspired composites is control over composition, gradients, interfaces, microstructures, morphology, and responses under dynamic conditions. In certain instances, synthetic composites are superior, for example, in the automotive and aerospace field where temperature resistance is critical. Yet, bioinspired composites can be produced under eco-friendly conditions by incorporating traditional design strategies and advanced synthetic materials, resulting in exceptional properties. Studies on some of the most robust natural materials provide insights into basic principles, especially the critical role of molecular interactions and hierarchical architectures (Box 1a-f).[2,4] The structural hierarchy enables multiple deformation, self-healing, plasticity, and toughening mechanisms within the composites across length scales.[5] For example, at the nanometer scale (nm), architectures of compositional gradients and fuzzy interphases (3D interfacial regions), as discovered in layer-by-layer assembled structures, facilitate intrinsic toughening by chain slippage, stress delocalization, and non-destructive locking across organic interfaces. Simultaneously at larger scales of micrometers (μm), hierarchical structures play a pivotal role for extrinsic toughening such as crack-bridging and pull-out to dissipate energy via weak or soft interfaces (see fundamental relationships in Box 1g, h).[1,4] To harness such functions, many organisms have developed an unparalleled ability to shape mineral-rich materials into anisotropic structures to serve as load-bearing elements, which extend over several orders of magnitude in size.[6] The resulting combination of stiffness, strength, and toughness has fueled research for synthetic bioinspired analogs because existing synthetic composite materials often show increased strength at the expense of toughness or vice versa.

A second grand challenge in the modern materials world, which draws inspiration from nature, is that scale-up synthesis and processing yet have to be mastered in industrial settings, including the demand for added functionality on structural components.[7] Multi-functional hierarchical materials found in plants and living organisms include celluloses, keratins, and silk (Fig. 1, Box 1e, f). These complex systems in nature are produced at a massive scale and engineered using relatively simple building blocks and constituents under highly sustainable conditions, including aqueous environments and ambient temperature.

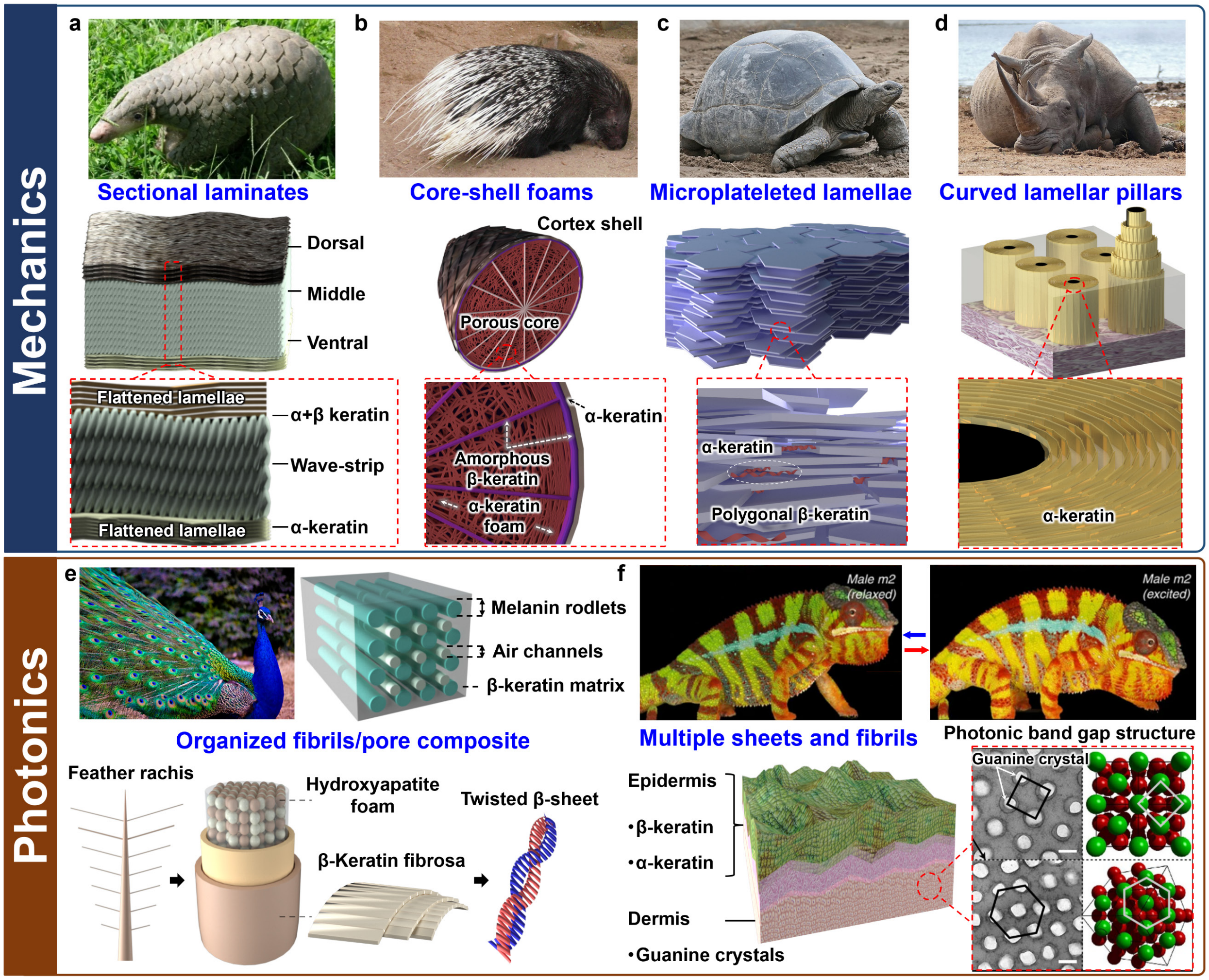

Figure 1 | **Keratin-based hierarchical structures in different animal species**. A common feature of keratin-based hierarchical composites are precisely folded tertiary keratin structures, which control mechanics by means of layers, interfaces, and gradients, as well as co-assembly with other functional polymers or minerals to generate periodic order. **a** | Pangolin scales consist of α-keratin and β-keratin and are known for their distinctive protection mechanism. The scales comprise of an internal layered structure with densely packed keratinized flattened lamellae that are wavy and parallel to the external surface in dorsal and ventral regions, and elongated cellular morphology that are tilted and deformed in the middle region.[8] **b** | Porcupine quills are composed of a keratin configuration that includes a stiff outer sheath and compliant porous core structures.[8] **c** | Turtle shells are biomineralized structures constructed with compacted, ordered, and stacked polygonal keratin micro lamellas that have a high amount of β-keratin and a small quantity of α-keratin and minerals (calcium phosphate and calcium sulfate).[9] **d** | Rhinoceros horns are made of α-keratin with a lamellar structure (2–5 μm in thickness) stacked in the radial direction with tubules (40-100 μm in diameter) dispersed between the lamellae, extending along the length of the horn in the growth direction.[10] **e** | Peacock tail feathers are composed of parallel melanin rod bundles connected in a β-keratin matrix for 2D photonic structures, which generate magnificent iridescent colors. The feather's rachis contains branches of multi-colored barbs that derive their unique iridescence from parallelly oriented bundles of fibrils composed of two twisted β-sheets that consist of mostly hydroxyapatite foam and a small portion of cortex from β-keratin fibers.[8] **f** | The panther chameleon shows a beautiful green striped color pattern due to guanine photonic crystals in the relaxed state. These colors change to a bright yellow in the stressed state. The epidermis consists of highly keratinized layers of α-keratin and β-keratin, which give a rough texture on the skin, defend against predators, and protect the softer and more adaptive photonic crystals underneath the epidermis (scale bars are 200 nm).[11]

We specifically highlight keratin, a critical component of many natural structures, as an inspirational source (Fig. 1).[8] Keratin is a structural protein in hair, horn, and hoof (Box 1f) that serves as a robust yet soft material in the exoskeleton of a wide range of vertebrates (Fig. 1). The exoskeleton of animals exhibits multiple functions: self-defense, communication, sensing, and temperature regulation, albeit each process uses different mechanisms facilitated by complex hierarchical structures and composition gradients. We categorize examples of these keratin-based multi-functional hierarchical structures from six distinct animal species based on their two primary functions: mechanics and photonics (Fig. 1). One major function of horn and hoof is impact resistance and energy absorption.[12] More subtly, keratin functions as defensive shielding in the skin via a complex curved architecture in pangolin scales (Fig. 1a),[8] a piercing weapon in porcupine quills (Fig. 1b),[8] sturdy protection via ordered stacks in turtle shells (Fig. 1c),[9] and in rhinoceros horn (Fig. 1d).[10] These hierarchical structures vary in their shape from waved stripes of cellular morphology in multilayered laminates (Fig. 1a) to amorphous foams (Fig. 1b), to microplatelet-containing lamellae of turtle shells (Fig. 1c) and curved lamellar pillars in rhinoceros horns (Fig. 1d). All these hierarchical structures achieve the function of dissipating energy for self-defense. In one specific structure, the pangolin scale's multilayered laminates, the lamellar structures exhibit unusual crack deflection with non-uniform crack profiles (Fig. 1a). Interlamellar shearing of the keratin interfaces leads to tablet sliding and inelastic regions surrounding cracks, resulting in enhanced fracture toughening.[13] The microtubule structures serve as a stiff reinforcement that supports the entire wall and prevents catastrophic failure under impact loading via inherently viscoelastic properties of keratin.[12] These hierarchical layered architectures are necessary for penetration-resistance and dissipating energy within the sub-layers, helping to delocalize stresses and damages while being environmentally resilient under extreme fluctuations in humidity and temperature.

In contrast to direct structural applications related to self-defense, keratin can be combined with periodic inclusions of melanin rods to form photonic crystals with the bright, vivid coloration found in many bird's feathers, including peacock feathers (Fig. 1e). Keratin can also provide structural protection of guanine nanocrystals for color adaptivity in the chameleon dermis (Fig. 1f).[11] Both of these photonic structures employ fibrillar architectures, as seen by organized fibrils and pores in peacocks' feather frames (Fig. 1e), as well as multiple sheets and fibrils in chameleon skin (Fig. 1f). These complex keratin-based hierarchical structures illustrate examples of multifunctionality, while being mechanically resilient,[12,13] fulfilling essential roles for defense, stress signaling, courtship display through structural color, and thermal protection.[11]

Elucidating the underlying mechanisms and correlated functions of such complex structures still poses a tremendous challenge for the scientific community. Understanding the design principles provides opportunities to incorporate various functions in synthetic systems such as photonics and morphing while enhancing mechanical integrity. The goal of 'emulating nature's design principles' can also be accelerated through interactive, real-time feedback in synthesis and characterization by utilizing opportunities in machine learning (ML), data science, artificial intelligence (AI), and additive manufacturing (AM).

Based on structure-function prototypes found in nature and recent studies, this review examines recent breakthroughs, trends, and advances in the design, synthesis, and understanding, of nature-inspired hierarchical bioinspired materials. We emphasize on how weak and strong chemical interactions can be configured to create synthetic hierarchical architectures with tight control over morphology, structure, function, appearance, and mechanics at different length scales, across time scales, and force scales. We identify critical challenges for designing future structural materials with added functionalities and discuss how an interdisciplinary era of materiomics, that harnesses big data, could accelerate the development of the next generation of advanced materials by linking material structure to properties and functions.

2. Hierarchy of interactions and energy across scales

The unique combination of mechanical and functional properties in natural materials is associated with the hierarchical organization at various length scales, that can also change with time, from molecular ordering to macroscale assembly (Fig. 2, Hierarchical structures). Such synergetic self-organization is mediated by ubiquitous, highly structured, hard-soft interfaces.[14] A common feature of these interfaces is 'deliberate imperfection,' i.e., a designed degree of complexity not found in engineered materials.

The spatial dimensions of hierarchical structures vary greatly depending on end-goal functionality and volume constrains from 0 dimensions (0D) to *N* dimensions (*N*D). *N*D may also incorporate further dimensions such as time or other responsive changes in the material. The dimensions of these *N*D structures further influence the size and subsequent interactions of the molecules and interfaces and the eventual, multi-level, macro-scale material structure, such as twisted, laminated, or fibrous composites (Fig. 2, Hierarchical Structures). Hierarchical structures can span beyond singular dimensions, evidenced by the organization of peptides into nanoscale sheets and their subsequent organization into fibrillar structures that bundle to form large-scale fibrillary and laminated solids (Fig. 2, Hierarchical structures, a-e). The assembly into laminated and fibrillar structures defines a higher level of organization of interfaces and nanostructures in large-scale bioinspired and synthetic inorganic-organic materials (Fig. 2, Hierarchical structures, f-n).

Ultimately, the combination of strong and weak interfaces determines the toughness, strength, and stiffness of a material, along with its shear and adhesive properties (Fig. 2, Global functions, two top panels). A prominent example from nature that employs strong and weak interfaces for energy dissipation is nacre, which features a "brick-and-mortar" configuration with relatively stiff aragonite bricks and soft biological material as the mortar. A small fraction (~5%) of protein binder is sufficient to significantly increase fracture toughness as it allows the aragonite bricks to slide, dissipating energy while retaining the overall high stiffness.[15] Reversible reorganization of interfaces, driven by induced phase and molecular transformations, facilitates a dynamic behavior that allows nature to modulate shape and stimuli-responsive properties (Fig. 2, Global functions, two bottom panels). Morphing and responsive behavior are realized by a variety of molecular mechanisms, such as re-alignment or re-bonding of functional groups, molecules, and nanoparticles. The processes of bonding, reactions, relaxation, and diffusion of structural elements range from picoseconds to millisecond timescales (Fig. 2, Time scale and interactions). Furthermore, materials-forming processes include aggregation, crystallization, dissolution, phase separation, relaxation, controlled deformation, appearance, morphing, and self-healing of hierarchical materials across similar time scales.

Therefore, it is challenging to develop synthetic hierarchical structures with the mechanical resilience (Box 1g) and functionalities that nature can offer.[16] It remains difficult to re-create and program the complexity of diverse components and interfaces, which combine different phases, create material gradients, and enable reversible energy dissipation, with incredible control over local and global mechanics, into synthetic processes. We will examine the processes through which materials acquire multiple functionalities in the next section.

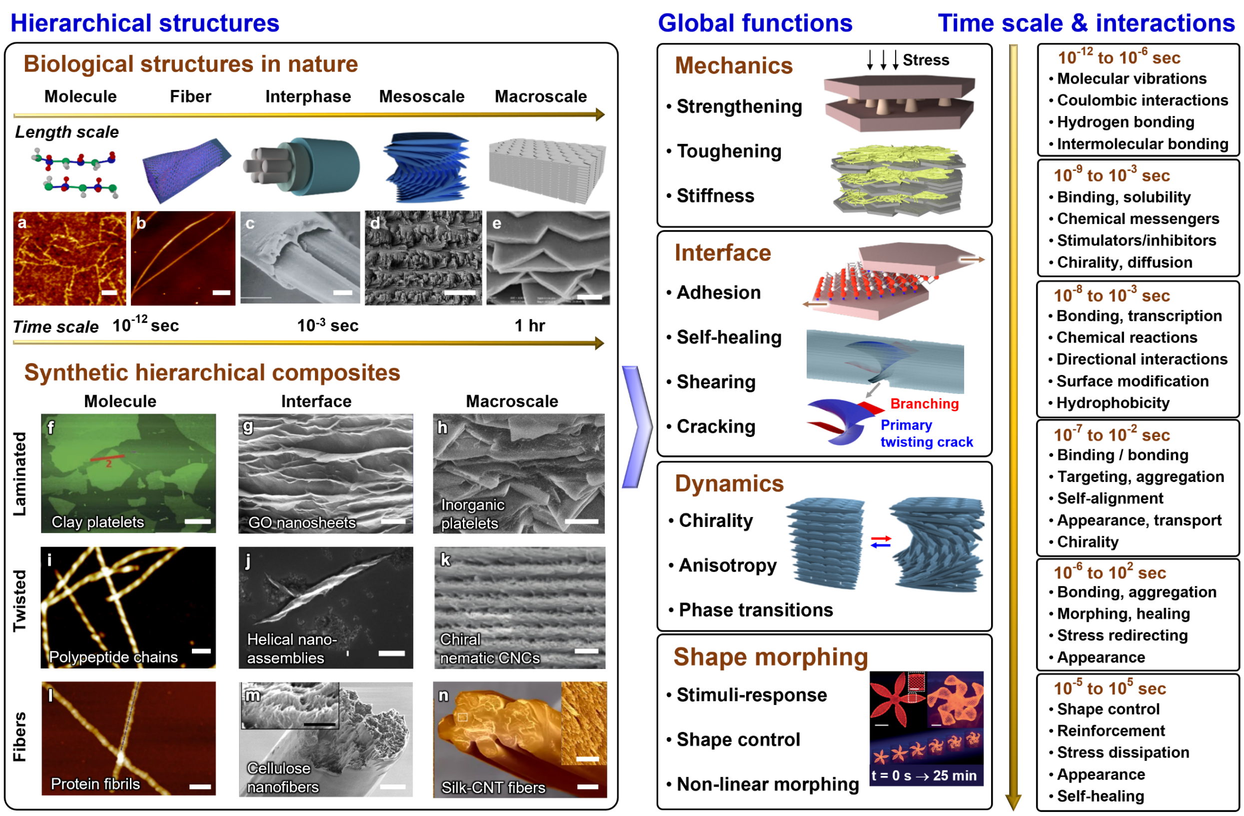

Figure 2 | **Hierarchical bio-inspired composite designs in terms of spatial and time scales and major contributions in mechanical functionality.** Representative hierarchical biological structures from nature, schematics (top panels) and actual morphologies including, **a** | AFM topographical image of β-sheet secondary structure of silk fibroin (scale bar is 50 nm),[17] **b** | AFM topography of silk nanofibrils (scale bar is 0.5 μm),[18] **c** | SEM image of single-filament silkworm silk fibers (scale bar is 5 μm),[19] **d** | SEM image of hierarchical Bouligand structure of the dactyl club of the stomatopod (scale bar is 20 μm),[20] **e** | SEM cross-section image of natural Cristaria plicata nacre with hierarchical layered microstructure (scale bar is 1 μm).[21] Synthetic and hybrid composite materials morphologies include **f** | AFM image of polyvinylalcohol (PVA) coated core-shell clay nanoplatelets (scale bar is 1 μm),[22] **g** | SEM image of layered nanostructure of graphene oxide (GO) sheets combined with silk fibroin (scale bar is 600 nm),[23] **h** | SEM image of artificial hybrid nacre materials with laminated clay-biopolymer composite microplatelets with highly ordered "brick-and-mortar" arrangement (scale bar is 1 μm),[21] **i** | AFM image of twisted amyloid fibrillar bundles (scale bar is 100 nm),[24] **j** | SEM image of right-handed helices self-assembled from *D*-cysteine-stabilized CdTe nanoparticles (scale bar is 100 nm),[25] **k** | optical microscopy image of a hierarchically organized cellulose nanocrystal (CNC)-polysaccharide composite with periodic helical organization and sub-micron pitch length (scale bar is 10 μm),[26] **l** | AFM image of silica deposited protein core-shell nanofilaments (scale bar is 50 nm),[27] **m** | SEM image of nanostructured artificial cellulose nanofibrils with anisotropic arrangement visible in fractured areas (scale bar is 200 nm),[28] **n** | SEM image of as-spun regenerated silk/CNT fibers (scale bar is 20 μm).[29] The hierarchical structure translates into global functions, utilizing a range of time scales and characteristic interactions for each order of magnitude (right hand side).

3. Synthetic and bio-inspired materials and structures

In the following, we survey examples of current, state-of-the-art approaches to design, assemble, and understand composite materials with elements of hierarchical organization, followed by a global analysis and categorization of mechanical performance relative to traditional composite classes.

3.1. Shape-morphing composites with *N*D functionality. Responsive bio-inspired composites are based upon general principles of creating interfacial stresses, with the inclusion of dynamically responsive elements for active transport, self-healing, touch sensors, tunable photonic structures, and shape morphing observed in nature (Fig. 2 Global Functions bottom panel and Time scale & interactions).[30] Volume may change or be conserved in this process, like in sea cucumber (*Holothuroidea*) or Venus flytraps (*Dionaea muscipula*) morphing.[31] Hierarchical metamaterials utilize both active and passive mechano-functionality in response to external stimuli to achieve *N*D functionality. Active mechano-functionality, such as muscles or actions that require energy, corresponds to environmental stimuli responses, such as reversible shape transitions or color changes. In turn, passive functionality originates from within biological assemblies. Bonds and molecules can rearrange themselves when exposed to external environmental stimuli while not actively utilizing energy to react. Examples include the sorption-induced bending of wood and the curling of hairs in response to heat.[32]

One classic example of active bioinspired materials includes dynamic bilayer hydrogels, composed of cellulose fibrils embedded in a soft matrix that enables morphing in wet environments via encoded anisotropic swelling through the pre-programmed fibril orientation.[33] More complex shape transformation (e.g., helicoidal) can be achieved by controlling interfacial stresses in the bilayer structures depending on the swelling ratios and elastic moduli. For example, the aspect ratio of silk bilayer nanosheets can control biaxial stresses and self-rolling into different tubular shapes.[34] Engineered structures with pre-programmed elements, sometimes instituted using kirigami/origami, can show organized transformations due to complex buckling and adaptive architectures, and adjust their shapes for complex morphing.[35] The so-called 4D behavior with time as additional axis emphasizes the unique, diverse real-time behavior of the structures. This direction in research is explored, for example, in silk-based patches for tympanic membrane repair,[36] as well as in soft robotics, which needs special attention beyond the scope of this review.

3.2. Laminated layered composites beyond nacre. Layered bioinspired materials from graphitic, cellulosic, and other nanomaterials have been produced to mimic and surpass natural nacre composites, in some cases resulting in impressive materials performance and functionalities unseen in traditional laminates (Fig. 2e-h).[16,37,38] A relatively low volume fraction of reinforcement material in a brick-and-mortar structure can achieve high fracture toughness similar to that of nacre, such as 3.4 $MPa \cdot m^{-1/2}$ with 38 wt% clay in PVA composites (comparable to nacre at 4-8

MPa·m$^{1/2}$) (Fig. 2f).[15] PVA hereby increases the composite's energy dissipation. Tougher materials have been designed by alternatively stacking microplatelets with similar dimensions to those of aragonite used in nacre between thick chitosan layers.[39,40] Microplatelets can be decorated by nanoparticles and sintered to adjust the size of asperities and mineral bridges, facilitating resistance to sliding (Fig. 2f-h and Global Functions, top two panels). Engineering of non-platelet functional particles, including hydroxyapatite[41] and zirconia polycrystals,[42] might involve rotation for energy dissipation as a toughening mechansim.[43]

A strong interface is critical for effective load transfer and energy dissipation as demonstrated in the early studies using layer-by-layer assembled composites; however, the interface also needs to be compliant to deflect cracks and delocalization stresses. The complementary pairing of polymers with inorganic fillers is characterized by the superposition of multiple types of interfacial interactions that differ in strength and dynamics. Adding polymers to control relaxation dynamics is considered an effective toughening method.[22,37] Exceptional values in strength and modulus can be achieved in composites with high inorganic phase content (above 90%), contributing to stiffness that increases intrinsic toughening via crack deflection. Necessary interfacial interactions can be tailored via nanosized building blocks during biomineralization.[38,42] An aspect that has often been overlooked is the biochemistry of proteins that serve as essential building blocks or templates that accurately regulate biomineralization. For instance, with recent advances in RNA sequencing and high-throughput proteomics techniques, one can reliably design full-length sequences that bear additional reinforcement potential.[44]

In another high-performance synthetic nacre, the interlayer polymer is a blend of a chitin/silk fibroin matrix and acidic proteins, which provides a robust interface and a unique interlocking mechanism while facilitating large shear deformation and strain hardening in the polymeric phase.[45] In this manner, the combination of nanofibrous materials with 2D nanosheets is an efficient option for synergetic strengthening.[46] A recent breakthrough involves the design of interfaces that enable large-scale sliding of tablets in engraved glass laminations, leading to up to more than double the toughness of tempered soda-lime glass and more than triple the toughness of PMMA (plexiglass).[47] The uniform plate geometry and patterning avoid strain localization and maximize energy dissipation. However, at the next level of hierarchy, additional complexity like symmetry-breaking alignment and correlated twisting in stacks must be introduced to enhance mechanical performance.

3.3. Twisted laminated Bouligand and chiral composites. Another class of laminated materials features organized twisted stacking with a slight rotation and twisting angle per layer, commonly referred to as Bouligand structure (Fig. 2d).[48,49] As seen in mollusk shells and arapaima fish scales in nature, these twisted hierarchical structures demonstrate a remarkable strength and toughness to resist compression and penetration damage.[50] The unusual toughening mechanism arises from multiple layers in the hierarchical architecture. For example, a mineralization gradient created by a helicoidal arrangement in a herringbone superstructure deflects and twists crack propagation. The striated region consists of circumferentially oriented fibers and exhibits impressive compression during impact and exceptional toughness during stretching.[51] Furthermore, double-Bouligand structures have been found to support mechanical robustness, for example, in the stomatopod dactyl club.[52]

These superstructures with unusual performance are a great inspiration for synthetic hierarchical chiral and twisted materials. Various top-down micro/nanofabrication techniques have been explored, including electrochemical deposition and direct laser writing.[53] Precise control of hierarchical structures from the nanoscale to the macro-scale and large-scale fabrication are still a challenge, however. Hereby, bottom-up strategies using directed assembly of individual entities could provide a faster solution. Better precision at the local level was achieved by controlling the surface chemistry, geometry, and dimensions that enable fast "construction" of arbitrary geometries and richer possibilities to integrate additional components (Figure 2i-k).[54] Traditional liquid crystals (LC) with chiral nematic (cholesteric) phases can be applied as templates, and a well-known example is the organization of polysaccharide nanocrystals, such as cellulose nanocrystals (CNCs) and chitin nanocrystals (ChNCs) derived from plants and crustaceans, respectively, into chiral nematic lyotropic LC phases.[55,56] Transparent films made from mixtures of wood and CNCs nanocrystals have reached strength similar to that of bone,[16] and helical organization in CNCs leads to selective color reflection of circularly polarized light (Fig. 2k).[57] Switchable lasers, controlled by relative humidity, have been recently built from plant-based CNCs and fluorescent polymers at room temperature.[58]

In silico studies of the behavior of the Bouligand shell and thin film structures reveal a multitude of mechanisms for coping with mechanical impact.[52] Depending on fiber material properties, Bouligand structures can result in band gaps that promote impact tolerance and facilitate the propagation of deformation waves, resulting in energy redirection and better performance at high strain rates. Experiments demonstrated crack twisting and distributed damage mechanisms with greater energy dissipation due to the minute differences in fiber orientation and reduced delamination. Twisted laminated structures drive the crack path in tortuous trajectories around designed heterogeneities.[50,59] These techniques found in nature are applied in engineered heterogeneous materials, like some types of ceramics and ballistic armor, that drive the crack path in tortuous trajectories governed by heterogeneities. The functionality of Bouligand structures finds uses in optics, acoustics, and mechanics; however, current synthetic structural composites are not commonly tough unlike silks and other fibrous composites.

3.4. Fibrous and hairy nanoparticle composites. Fibrous composites are among the most sophisticated hierarchical structures in nature (Fig. 2a, b, l-m, Fig. 3). Silk, keratin, cartilage, and basal membranes are examples of an extraordinary class of natural nanomaterials that exhibit unparalleled mechanical performance and additional functionalities, such as ion-selectivity essential for applications in numerous energy technologies.[60-62] Silks from spiders' webs and cocoons have a wide variety of functions, ranging from absorption of the kinetic energy (spiders' webs) to the protection of larva (hard cocoon), and exhibit an increase in toughness at high deformation rate[60] and at cryogenic temperatures.[61] These unique combinations are possible due to the multi-domain architecture of silk proteins that control the energy dissipation mechanisms. Enhanced toughening in silks is governed by the stiffening mechanism of the individual fibrils with increased friction between them, resulting in resistive slippage and diverting crack growth (Fig. 3a),[61] akin to morphologies in CNT fibers.[63] Further toughening mechanisms observed in fiber composites include fiber pullout and fiber bridging, contributing to increased fracture toughness. At the molecular level, intrinsic toughening is linked to nanofibrils with a high degree of alignment (Fig. 3b). Furthermore, amorphous silk can convert into highly crystalline silk (Fig. 3c) by processing at temperatures above T_g, resulting in exceptional self-reinforced material properties.[64]

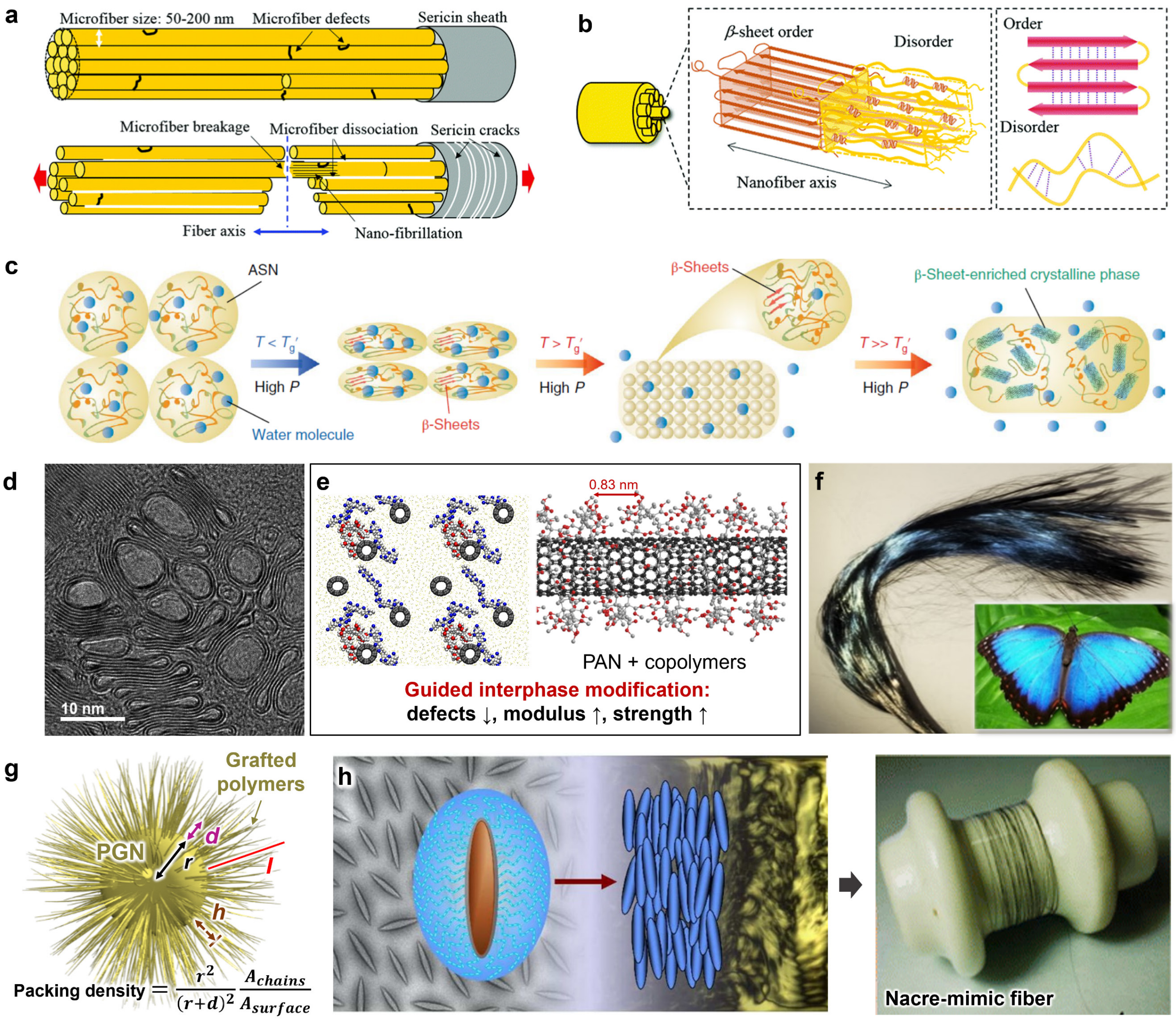

Figure 3 | **Fiber-based composites. a** | Schematic representation of the microfibers from *A. pernyi* silk (top) and the deflected fracture path that originated from a crack on the interface between sericin and the silk core (bottom).[61] **b** | The hierarchical structure of *A. pernyi* silk fiber. **c** | A proposed mechanism for the structural transition of regenerated amorphous silk during thermal processing.[64] **d** | TEM images of CNT based composites and carbon fiber.[65] **e** | Interphase modification through helically ordered wrapping of PMMA as well as of other polymers around single-walled CNTs increases alignment, modulus, and strength.[66,67] **f** | Surface-modified carbon fibers in polymer matrix demonstrating blue structural color.[68] **g** | The general scheme of polymer-grafted nanoparticles.[69] For a local radius of curvature of the particle *r*, the packing density of the polymer chains decreases for an increased, arbitrary distance *d* from the surface. The effective thickness of the polymer *h* is shorter than the extended chain length *l* and influences the interfacial properties. Inclusion of solvent and interdigitation with neighbor nanoparticles controls the toughening mechanism. **h** | An example of self-assembly of polymer-grafted hairy nanoparticles into fibers. The background (left) shows a TEM image of films of silica-coated α-Fe_2O_3 rods end-grafted with PMMA brushes,[70] which self-assemble in a good solvent such as toluene to form lyotropic nematic LCs as seen from polarized optical microscopy (right). The LC phases are enabled by tight control of the microstructures in PGN/polymer composites and facilitate spinning fibers with control over hierarchical architectures, dramatically enhancing both structural and functional properties. Similar processes are used to graft PAN to graphene oxide nanoparticles, using a precursor to spin nacre-mimetic fiber.[71] 2D materials such as graphene and MXenes,[72] or highly aligned 1D CNTs and CNCs with grafted polymers can also form functional fibers with properties depending on nanoparticle chemistry and shape.

Beyond natural fibers, carbon fibers are examples of ultra-strong and tough materials that exhibit exceptional modulus and strength per unit mass that places them in a special parametric space rarely achieved by other composites (Fig. 3d-f). Their current best performance stands at around 400 GPa modulus and 8 GPa tensile strength, while the theoretical limits remain at approximately 1000 GPa and 100 GPa, respectively.[73] Engineering the alignment of carbon nanotubes (CNTs) and polymer gel precursors as well as controlling defect formation is necessary to facilitate improvements (Fig. 3d, e).[66,67] For example, precisely tailored interfacial properties in CNT-polymer nanocomposites with polymethyl methacrylate (PMMA)-modified CNTs show up to 5x increase in tensile modulus and ~3x increase in tensile strength.[74] The inhomogeneity of carbon fiber surfaces also causes sp^2 and sp^3 carbon hybridization, which has been exploited to create *in-situ* polymerized hierarchical structures that exhibit structural color like that of butterfly wings (Fig. 3f).[30,68]

A new generation of synthetic composites involves polymer-grafted hairy nanoparticles (PGNs) (Fig. 3g, h).[75] PGNs are core-shell particles, where inorganic nanoparticle cores such as spheres, cubes, cones, rods, or sheets are directly linked with a shell of polymer chains using covalent or nonbonded interactions (Box 1a-d).[69] These core-shell architectures offer unprecedented opportunities to precision-tailor interphases. The volume fraction of the PGNs and the packing density of the grafted polymer chains can be controlled, including as a function of distance from curved nanoparticle surfaces, and entanglements with the polymer matrix control the toughening mechanism.[76] Particles with congruent geometry but having stiff spikes that replicate pollen and viruses also show unusual properties represented by anomalously high resistance against agglomeration and responsive behavior, as discussed in the next section.

3.5. Transcending design across different materials classes.

The selected examples of materials designs discussed above cannot reflect the rich variety of this field. We compare the enormous range of multifunctional attributes and mechanical properties realized in bioinspired composites to traditional engineering composites in the same parametric space in two corresponding Ashby plots (Fig. 4 and Table 1). The analyzed composites are color-coded according to their origin (biological or synthetic materials), type of morphologies (nacre-like, twisted, disordered, and cylindrical, fibrous microstructures), as well as parametric space occupied by traditional materials classes: ceramics, elastomers, metals, and fibrous composites (gray circles in Fig. 4).

Many engineering materials like carbon fiber polymer composites achieve high strength and stiffness, while aluminum has a lower strength and stiffness but high toughness and ductility.[3] When analyzing available materials data in terms of mechanical strength and elasticity (ultimate strength vs. ultimate strain), which is vital for practical designs of very strong materials with high resilience and non-brittle failure, we observe that known bio-inspired composites mostly occupy the same parametric space as traditional composite materials (Fig. 4a). The majority of known bioinspired composites with soft components such as CNT-silk and PVA-montmorillonite clay (MTM)-nano fibrillated cellulose (NFC) composites are comparable in ultimate strength to common engineered ceramics, polymers, and metals (~0.1 - 1 GPa) (Fig. 4a). Thereby, the strength of mineral or ceramic components, as well as that of the polymers can vary. The softer components, reconfigurable interfaces, and gradient organization facilitate higher deformability than synthetic composites, including maximum strains of 10%, and their ability to reconfigure from planar to highly curved or wrinkled, resulting in dynamic morphing.[34,69,75,76]

The strength of existing biological and bioinspired composites can match advanced synthetic fiber-based composites, e.g., when silks, keratins, and aramid nanofibers (ANFs) are combined with carbon nanotubes.[14,77] Beyond the elastic regime, yielding and strain hardening can result from local rearrangements such as disentanglement, strain-induced crystallinity, and chain slippage. Such processes add significant plasticity and result in ultimate strains of hundreds of percent. The combination of high ultimate strains with high strength in some wood-keratin composites sometimes surpasses that reported for synthetic fibrous composites (Fig. 4a). Second, if mechanical performance is considered in terms of toughness vs. stiffness (Young's modulus), biological and bio-derived composites (*i.e.,* those utilizing some quantity of natural materials) also perform like traditional composites (Fig. 4b). Bio-inspired composites dramatically extend the parametric space towards extremely compliant materials with uniquely combined high toughness and modulus, comparable to engineering polymers and ceramics (Fig. 4b). Some of these bio-inspired materials occupy valuable, non-traditional parametric space with extreme toughness, up to 100 MPa/m^3 for silk, chitosan, and wood-based composites, as well as high elastic moduli up to tens of GPa (Fig. 4b). Bioinspired composites can perform much better than regular elastomers/gels, showing high toughness values up to 10 MPa/m^3 (Fig. 4b). Specifically, silk-based and ANF-based composites can demonstrate high toughness while not venturing into the standard brittle fracturing regime (Fig. 4b).

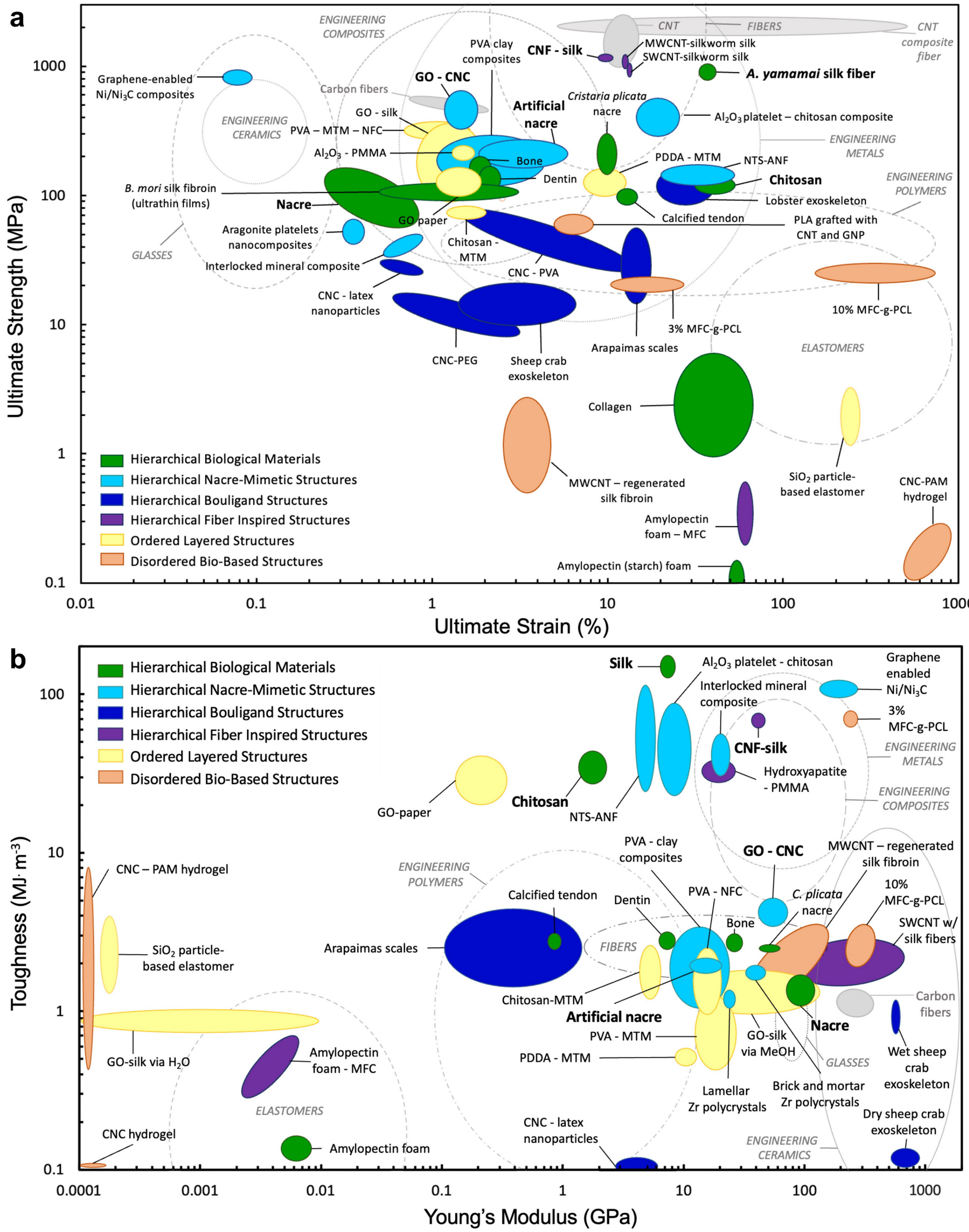

Figure 4 | **Analysis of mechanical properties of various composites in comparison with natural and traditional materials classes.** Ashby plots comparing **a** | the ultimate strength vs ultimate strain and **b** | the toughness vs Young's modulus for various hierarchical biological materials,[14,21,39,78-80] nacre-mimetic structural,[14,15,21,39,42,46,81-86] Bouligand structural,[59,87-91] circular hierarchical, fiber inspired structural,[14,41,77,80,83,84,92] layered ordered composites and random bionanocomposites.[23,38,39,79,81,84,92-98] The various strength, strain, toughness (work of fracture), and Young's modulus values are collected from tensile test data. The hierarchical materials (biological, nacre-mimetic, Bouligand, and cylindrical fibers) are included in green, light blue, dark blue, and purple, respectively. The ordered layered composites are in yellow and the random, disordered bio-based structures are included in orange. These materials are compared against common materials, included in light grey in the background, such as engineering metals (stainless steel, gold, copper, silver, tin, nickel, various alloys, titanium, Al/Si Carbide, zinc), engineering polymers (ABS, polycarbonate, polyamide, PEEK, polyethylene, PMMA, PS, PTFE, PVC, POM, polyester, epoxies, PLA), elastomers (butyl rubber, ethylene vinyl, natural rubber, polychloroprene, polyurethane, silicone elastomer), fibers (acrylic fiber, aramid fiber, cellulosic fiber, UHMWPE fiber, polyamide fiber), carbon fiber/carbon nanotubes (CNTs) and CNT composites, engineering ceramics (alumina, aluminum nitride, boron carbide, silicon carbide, silicon nitride, tungsten carbide, zirconia), glasses (borosilicate glass, glass ceramic, silica glass, soda glass), and engineering composites.[99-101] Hierarchically structured composites achieve the highest combinations of strength and strain, as well as toughness and stiffness. Hereby, composites that include biological fibrous components are among the best performing materials. Hierarchical microstructures imbue unique property combinations via weak and strong interfaces that improve the performance of soft component composites, as established in earlier sections, making them comparable to common inorganic engineering materials. High-end fiber-reinforced composites cannot easily be outperformed in terms of strength and ductility, yet engineering ceramics and metals like silicon carbide and titanium alloys are outperformed by CNF-silk, SWCNT/MWCNT-silk, and Al_2O_3-chitosan bio-inspired composites.[14,39,77] In these examples, exploiting silk's naturally high strength and ductility while incorporating stiff nanoparticles facilitates an intrinsic toughening mechanism.

Table 1 | **Details of the mechanical properties of different materials classes in Figure 4.** The table includes key mechanical properties for different material types, organized into the same groups and color codes as the Ashby plots in Figure 4. The categories include (1) hierarchical biological materials, (2) hierarchical nacre-mimetic materials, (3) hierarchical Bouligand structured materials, (4) hierarchical fiber inspired materials, (5) ordered, layered structured materials, (6) disordered, bio-based structures that can be used in common hierarchical materials, and (7) engineering materials. The data points for individual engineering materials subsets are not further detailed here and can be searched in the *CES Edupack* database[100] and in the reference by Ashby.[99] For some materials, the data were not directly reported in original works and are based on the analysis of tensile data and stress-strain curves using best estimates and error bars. The designation "~" indicates less certain estimates with high uncertainties.

Material Type	**Material**	**Ultimate Strength** (MPa)	**Ultimate Strain** (%)	**Toughness** ($MJ \cdot m^{-3}$)	**Young's Modulus** (GPa)	**Ref**
Hierarchical Biological	Amylopectin (Starch) Foam	0.170 ± 0.025	~62	0.18	0.0049 ± 0.0011	80
	Bone	150	1.75	~2.5	~25	39
	Calcified Tendon	80	12	3.9	0.7	39
	Chitosan	108 ± 15	42 ± 9	32 ± 9	1.9 ± 0.3	79
	Collagen	4.2 ± 3.3	46 ± 22	-	0.025 ± 0.023	78
	Dentin	105	2.5	2.8	7.5	39
	Nacre	95 ±35	0.7 ± 0.5	1.8 ± 0.5	90 ± 30	39,84
	C. Plicata Nacre	172 ± 50	0.9	2.4 ± 0.5	49 ± 11	21

	A. Yamamai Silk Fiber (Silk)	875	35	~150	~8.3	14
	B. Mori Silk Fibroin	100 ± 10	1.75 ± 1.5	0.328	7 ± 1	78
Hierarchical Nacre-Mimetic	Al_2O_3 Platelet-Chitosan Composite	315 ± 95	21 ± 5	41 ± 19	10 ± 2	39,84
	Aragonite Platelets-Organics Nanocomposites	64 ± 8	0.38 ± 0.07	-	-	14
	Artificial Nacre	267 ± 25	4 ± 2	2	18.6 ± 5	21
	Graphene-Enabled Ni/Ni_3C Composite	1022 ± 73	0.143 ± 0.02	110.2 ± 10	222 ± 10	85
	Graphene Oxide (GO)-Cellulose Nanocrystal (CNC) Composite	490 ± 30	1.1 ± 0.3	3.9 ± 0.5	54 ± 7	81
	Planar Mineral Composite of Aragonite Films in a Chitosan/Silk Fibroin Matrix	23 ± 2.8	~0.65	~8	~12	86
	Interlocked Mineral Composite of Aragonite Films in a Chitosan/Silk Fibroin Matrix	43.5 ± 4.5	~0.9	~30	~25	86
	Sodium Tetrasilic Mica - Aramid Nanofiber (NTS-ANF) Composites	130 ± 15	50 ± 24	67 ± 33	4.7 ± 1.7	46
	Polyvinyl Alcohol (PVA) - Montmorillonite (MTM) Clay Composites	170 ± 70	2.25 ± 2	~1.7 ± 0.6	17 ± 9	15
	Brick-and-Mortar Zr Polycrystals	-	-	~1.7	42 ± 4	42
	Lamellar Zr Polycrystals	-	-	~1.2	29 ± 4	42
Hierarchical Bouligand Structures	Arapaimas Scales (Dry and Hydrated)	~34 ± 17	~22 ± 14	~3.6 ± 2.4	~0.75 ± 0.65	59
	CNC-Latex Nanoparticles	25 ± 4	0.7 ± 0.2	0.1 ± 0.02	3.5 ± 1.5	90
	CNC-Polyethylene Glycol (PEG)	~13.5 ± 4	~2.5 ± 2	-	1.75 ± 1.25	88
	CNC-PVA Composites	57 ± 12	3.75 ± 3.25	-	~7.5 ± 4.5	89
	Lobster Exoskeleton (Dry, in Parallel and Transverse Directions)	~145 ± 35	~29 ± 16	-	4.7 ± 1.6	87
	Dry Sheep Crab Exoskeleton	12.9 ± 1.7	1.8	0.11	764 ± 83	91
	Wet Sheep Crab Exoskeleton	31.5 ± 5.4	6.4 ± 1	1.02 ± 0.25	518 ± 72	91
Hierarchical Fiber Inspired Structures	Amylopectin Foam - Microfibrillated Cellulose (MFC)	0.7 ± 0.25	60 ± 3	~0.5 ± 0.32	0.0046 ± 0.0025	80
	Cellulose Nanofibrils (CNF)-Silk Composites	1050	10	~65	~35	14
	Single-Walled Carbon Nanotubes (SWCNT) - Silk Fiber Composite	5.5 ± 4	2.3 ± 1	~2.3 ± 1	370 ± 300	92

	SWCNT - Silkworm Spun Silk Composite	785 ± 95	13.6 ± 1.2	6,600 ± 210	-	77
	Multi-Walled CNT (MWCNT)-Silkworm Spun Silk Composite	925 ± 145	15.5 ± 1.3	9,000 ± 4,500	-	77
Ordered Layered Structures	Al_2O_3-PMMA (Brick-and-Mortar)	200 ± 10	~1.4	-	-	82
	Chitosan-Montmorillonite (MTM) Composite	81 ± 12	1.9 ± 0.6	0.9 ± 0.4	6.1 ± 0.8	79
	GO-Silk Synthesized via H_2O	175 ± 75	0.7 ± 0.2	0.75 ± 0.25	0.005 ± 0.005	23
	GO-Silk Synthesized via MeOH	225 ± 75	1 ± 0.4	0.8 ± 1.5	75 ± 65	23
	GO-Paper	113 ± 9	0.3 ± 0.16	0.25 ± 0.1	32± 7	84
	PDDA-MTM	100 ± 10	10 ± 2	~0.5	11 ± 2	38,39,79
	PVA-MTM	150 ± 40	0.7 ± 0.2	~0.4	13 ± 22	38
	PVA-MTM Crosslinked with Glutaraldehyde (GA)	150 ± 40	0.33 ± 0.04	~0.5	106 ± 11	38
	PVA-Nanofibrillar Cellulose (NFC)	223 ± 31	~1.25	1.46 ± 0.59	~15 ± 5	96
	PVA-MTM-NFC	302 ± 12	~2	3.72 ± 0.63	22.8 ± 1.0	96
	SiO_2 Particle-Based Elastomer	~2 ± 1.5	270 ± 45	~3 ± 2	0.002 ± 0.0015	94
Disordered Bio-Based Structures	3% MFC-G-PCL	20.5 ± 3	450 ± 275	73 ± 3.3	0.245 ± 0.035	97
	10% MFC-G-PCL	24 ± 4.2	20 ± 5	2 ± 1	0.280 ± 0.075	97
	CNC Hydrogel	~0.03	~250	~0.04	0.005	93
	CNC-PAM Hydrogel	0.15 ± 0.07	716 ± 70	~1.6 ± 1	0.025 ± 0.007	93
	MWCNT-Regenerated Silk Fibroin	~1.5 ± 1	~3.0 ± 0.5	~1.9 ± 1.4	~ 0.07 ± 0.05	95
	PLA Grafted with CNT and GNP	66 ± 11	6.0 ± 1.1	-	2.1 ± 0.5	98
Engineering Materials	Elastomers	27 ± 25	610 ± 340	0.75 ± 0.45	0.024 ± 0.02	99,100
	Engineering Ceramics	550 ± 450	0.12 ± 0.6	4.5 ± 3.5	700 ± 500	99,100
	Engineering Composites	1050 ± 950	5.5 ± 5	48 ± 43	110 ± 95	99,100
	Engineering Metals	1210 ± 1000	40 ± 39	75 ± 65	205 ± 190	99,100
	Engineering Polymers	60 ± 54	401 ± 400	5.1 ± 5	5.1 ± 5	99,100
	Fibers	2000 ± 800	19 ± 17.5	2.5 ± 0.9	70 ± 68	99,100
	Carbon Fibers	680 ± 40	1.4 ± 0.6	1.05 ± 0.15	45 ± 13	100
	Carbon Nanotubes (CNT)	1600 ± 500	10 ± 1	-	-	100
	CNT Composite Fiber	1800	355 ± 345	-	80	101
	Glasses	1000 ± 980	0.14 ± 0.10	1.0 ± 0.5	80 ± 20	99,100

Overall, we can conclude that the expansion of characteristics of bioinspired composites into high performance space with extremes beyond traditional metal and ceramic composites is possible, especially if we consider specific features normalized to material density. However, a deeper understanding of the principles behind hierarchical structural and interfacial organization is required.

In addition, the characterization of hierarchical materials is challenging and benefits from advances in multiple areas that are not further reviewed here. Critical techniques include scanning probe microscopy (nano-DMA, AFM-IR, AFM-Raman), high-resolution electron microscopy (HR-TEM, STEM, EELS), synchrotron X-ray/neutron scattering, nano-X-ray computed tomography, advanced spectroscopy, as well as *in-situ* real-time monitoring of mechanical properties and dynamic changes in local chemical and morphological features, under ambient conditions, in a fluid environment, and at elevated temperatures.

4. Modeling and simulation of hierarchical materials properties

Modeling and simulation of mechanical and other functional properties can guide the design of bioinspired hierarchical structures within an unlimited space of chemistry and assembly across scales. Simulations typically rely on inputs from experimental data, experimentally inspired data, and specific algorithms to calculate sophisticated properties. Knowledge is generated by analyzing the computational results and comparisons to experimental data, extending material screening to hypothetical model structures and property predictions in iterative feedback loops.

Typically, simulations employ individual techniques suitable for specific length scales while the integration across hierarchies remains difficult (Fig. 2).[102,103] *Ab initio* electronic structure simulations, such as Density-Functional Theory (DFT), are typically used for a few hundred atoms to investigate geometries, transformations in chemical bonding, cohesive energies, band gaps, and elastic moduli, limited to picosecond dynamics and excluding electrolytes. As an example, DFT calculations can forecast the strength of cross-links between fillers and polymer matrices (Fig. 5a).[104] The information can then be used to assess the mechanical strength of covalently bonded composites via reactive MD simulations and identify parameters for better reinforcement, such as the diameter of CNTs, the role of defects, and suitable polymer chemistries.[105] At the next level, atomistic Molecular Dynamics (MD) simulations can be applied up to a million atoms and dynamics up to microseconds. Metrics of performance include accurate representations of chemical bonding, the structure (e.g., lattice parameters), surface energies, solvation energies, and mechanical properties (see also Box 1).[106] All-atom MD simulations have explained, for example, up to 80% reversible actuation of β-DNA attached to gold nanoparticles in agreement with experiments on the ~10 nm length scale (Fig. 5b). Structural changes occur in response to the addition of ethanol and variation in the local dielectric constant,[107] as well as upon the addition of multivalent cations that modify the ionic strength.[108] Thermodynamically consistent force fields such as the INTERFACE Force Field[106] allow the analysis of inorganic-(bio)organic materials, including binding energies, interfacial shear strengths, and glass transition temperatures in about ±5 K agreement with experimental data (Fig. 5c).[109] Effects of conformations, electrolytes, and assembly preferences during processing can be monitored in atomic resolution, which is typically not feasible in experiments and supports the design of *N*D functional bio-inspired materials.[66]

Limitations in the size of all-atom models on the order of 100 nm and in dynamics on the order of 1 μs can be overcome by coarse-grained (CG) simulations, which sacrifice most chemical detail and can explore between 10 to 100 times larger spatial and temporal scales.[102] CG MD simulations have illuminated the role of interphase regions in nanocomposites (Fig. 5d).[76] In polymer-grafted "hairy" nanoparticles, for instance, a relatively low grafting density and high length of surfactants was shown to enable significant interdigitation of the modified nanoparticles and improvements in mechanical properties (Fig. 5d).[75,76] MD and CG methods also uncover scaling relations and provide data to train ML algorithms for accelerated property predictions (Box 2).[110] At scales beyond micrometers, the mechanical response of composite materials can be effectively analyzed using peridynamics simulations, phase field models, and the finite element method (FEM).[111] Peridynamics models involve bonds inside the material and mimic associated deformations (Fig. 5e).[112] Peridynamics is well suited to simulate heterogeneous fracture evolution of polymers, including elastic and plastic deformation, unguided crack nucleation and growth, and crack branching at interfaces. Alternatively, phase-field models can be employed which assume a continuum representation and a specific parameter that represents the progress of fracture at every point in the specimen. FEM simulations of fracture can be challenging due to the presence of ubiquitous matrix/inclusion interfaces and complex geometries that defy the underlying continuum assumptions. Hereby, atomistically-informed FEM simulations can overcome some of these challenges (Fig. 5f, g)[113] and have been helpful, for example, to analyze crack twisting and distributed damage mechanisms in Bouligand structures to explain increased energy dissipation before failure and promote impact tolerance.[114] Band gaps and wave filtering capabilities could also be identified as a function of the fiber material and orientation (Fig. 5h).

In summary, routine simulations are currently feasible in selected areas on the time-length continuum and provide guidance on specific aspects of composites (Fig. 2, right column). Some methods are also frequently used in combination (MD/DFT, CG/atomistic MD, FEM/MD).[102,111] Grand challenges include better representation of structure-function phenomena across different length scales and new approaches to predict the behavior over long-time scales. Fracture mechanisms of bio-based materials are largely an open field as they have been far less studied than those of less heterogeneous materials. Specifically, the prediction of tortuous fracture in combined soft and hard material components remains a very challenging problem.

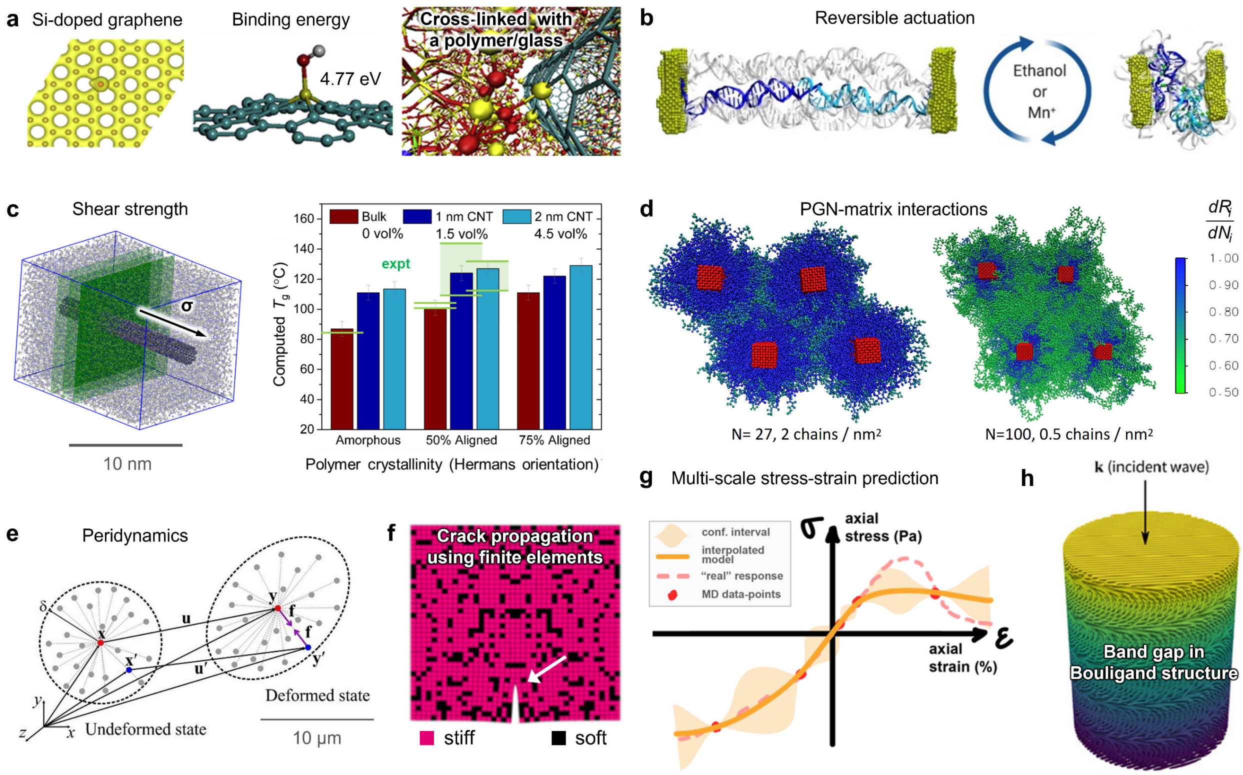

Figure 5 | **Insights into the function and mechanics of bioinspired composites by modeling and simulation**. **a** | Electronic structure of local Si-defects in graphene and calculation of a C-SiH bond energy using DFT. Subsequent all-atom MD simulations of cross-linking on CNT surfaces can guide experiments to optimize bonding to polymer matrices.[104,105] **b** | Functionalization and up to 80% reversible actuation of gold nanostructures modified with DNA, induced by changes in solvent or ionic concentration according to all-atom MD simulation.[107,108] **c** | MD simulations of shear strength and glass transitions in PAN/CNT composites. Glass transition temperatures reveal ±5 K agreement with experimental data. The molecular origin of T_g, the influence of CNT bundling and of CNT volume fraction could be identified.[109] **d** | Hairy nanoparticles support non-covalent mixing with a polymer matrix (green), whereby the packing density and chain length of the "hairy surfactants" (blue) has a critical influence on the composite properties, shown by coarse-grain MD simulations.[76] With the advancement of reliable all-atom force fields[106] and larger-scale coarse-grain models,[111] it is possible to predict the role of nano- and microscale features such as packing, defects, and interfaces on macroscale properties. **e** | In peridynamics, bond lengths and bond failure are monitored to compute continuous deformation and stress-strain characteristics at the microscale. **f** | Simulation of crack propagation in a FEM simulation (see arrow).[115] **g** | Results of multiscale simulation of the mechanical response of a graphene/epoxy composite. From a large set of data-points from all-atom simulations and narrowed confidence intervals, Gaussian process regression was used to construct a surrogate continuum model to predict the stress distribution from the mechanical state (current strain) for time-independent systems.[113] **h** | Multi-scale simulation of the band gap in Bouligand structures of a transversely isotropic material using finite elements up to the micrometer scale.[114]

5. Trends, broader impacts, and future developments

Applications of bioinspired composites range from drug delivery, wearable electronics, and human-computer interfaces to structural components for the automotive and aerospace industries. The multifunctional attributes imply a unique combination of properties, including mechanical robustness, flexibility, transparency, sensing, adapting (morphing), optics (photonics), electrical and thermal conductivities.

5.1. Developing ambient bio-synthetic processing techniques. There is a good, albeit still incomplete, understanding of the fundamental building blocks of biological structures. In most cases, it is still unknown how nature goes from the building blocks to the final, complex hierarchical structure, creating a need to better understand biogenesis or "biofabrication" of materials. There are a few well-studied exceptions, such as the biotechnological production of engineered silk fibers.[116] Recent breakthroughs also include understanding of the biofabrication of mussel fiber adhesives[117] and of the development of complex hard tissues such as the stomatopod dactyl club (Fig. 2d).[51] However, many intriguing questions remain. For example, the evolutionary principle behind the prevalence of Bouligand structures in biological materials, structure-mechanical property relationships of the twisting angle, and the relative significance of the contribution of material building blocks to the material architecture remain unclear.

Amongst novel material design methods, digital manufacturing such as 3D printing combined with advances in artificial intelligence is rising in prominence due to its ability to create highly complex structures. For example, additive biomanufacturing using silk dopes can preserve natural, sustainable, green, and aqueous processes while exploiting new additives, such as aramid nanofibers and other emerging nanofibers from recycled plastics and applications.[118] Advances in the addition of other polymers, inorganics, sequestration of bioactive components, the use of microfluidic devices for processing, subtle changes in pH value and electrolyte composition, as well as sampling the space of processing parameters, offer a suite of new options for 3D printing of hierarchical bioinspired materials. Target properties may include, for example, optical clarity, loading with bioactive components, and tunable mechanical performance.

Remarkably, all structures discussed here from natural materials are only derived from aqueous-based synthesis and assembly processes conducted at ambient temperature and pressure. When these amazing material outcomes and functional features are considered in the context of using benign conditions to drive material assembly, emulating such systems for our future material needs becomes even more compelling and amplified in importance. New ways to apply environmentally friendly processing as we move to the next generation of processing technologies and bio-inspired material systems would bring enormous benefits in sustainability to our planet.

5.2. Accelerated design using data science and machine learning. Tremendous innovation and acceleration in precision engineering of nature-inspired materials for targeted functions can be expected by integrating experiments with theory, modeling and simulation, data science, and artificial intelligence tools (Box 2a).[115] While structural order at specific length scales has been experimentally demonstrated in synthetic composites, structural hierarchy across multiple length scales remains lacking to-date and may be achieved sooner using such convergent techniques. Simulation and data-driven methods, complemented by mathematical approaches, such as category theory, can link the physiochemical properties, characteristics, and function of a material.

The synergy of these approaches introduces a new field of materiomics, which aims at ordering the vast materials space and accelerating materials design in a unified manner (Box 2b, c).[103,110]

Specifically, ML algorithms can accelerate materials discovery as follows.[115] Large training sets of data using features of the electronic, atomic, or microscopic scale and known mechanical and other physical properties can be used to train neural networks such as graph neural networks (GNNs) and convolutional neural networks (CNNs) for learning and connecting structure-property relationships.[119] The models can then make property predictions for untested structures and help to optimize synthesis and design (Box 2a, b). Novel capabilities in materials design also emerge using graph-theory (GT) based descriptions of nanocomposites, which can capture the networked structure of nanofiber reinforcements.[120] Concepts from visual art and music have been combined with AI to navigate the vast space of protein sequences.[121] The rapidly growing amount of data from high-throughput experiments and simulations also benefits from the organization in databases and multidimensional analysis with consistent and statistically robust content (Box 2c). A bottleneck is often the extraction of relevant data for a given problem from the literature, which may encompass hundreds of thousands of prior publications and could be accelerated by advances in information retrieval and natural language processing.

Data science also provides tools to better connect high fidelity modeling and simulation across different scales. Specific chemistry knowledge has been precisely translated into nanometer-scale models and force fields to carry out predictive MD simulations.[103,106] Nevertheless, capturing *any new chemistry* and *the effect from the atomic scale to microscale deformation and fracture behavior* in models remains a grand challenge. Obstacles involve (1) quickly and accurately parameterizing new chemistry and (2) effectively passing information from atomistic models to coarse-grained models and continuum representations. In addition, uncertainties in experimental nanoscale mechanical characterization of soft materials add complexity in providing guidance and validation for modeling. Data science and machine learning methods are promising to perform the necessary dimensionality reductions of structures and of interaction energies between particles and domains upon entering larger scales (Box 2d).[122] Such tasks can be achieved in uniform ways by employing hierarchical graph encoders and decoders, whereby chemical identity, geometry, and topological patterns play a critical role, similar to those explored earlier for multiscale simulations in adaptive resolution.[102] ML techniques may also be adjusted to enforce certain principles such as a Hamiltonian system if used to substitute physics-based simulations. Community-wide efforts to standardize reference states, key properties for validation, protocols for simulations, and open documentation of ML algorithms would enhance reproducible usage and integration of computational methods by the experimental community.

5.3. Future trends and impact. Nature is highly efficient in designing materials with unique optical, mechanical, and other functional property combinations through distinctive processing techniques. The integration of experimental and theoretical work can uncover new classes of bio-inspired materials that can enormously impact society through a unique amalgamation of properties. Modeling techniques including multiscale simulation, AI/ML, and materiomics may reveal hidden opportunities for designing multifunctional materials with high strength and toughness at faster development rates with sustainable routes, increasing the efficiency of material design. However, challenges remain in fulfilling the demand of these bio-inspired composites for high-performance applications such as aerospace composites, where extreme temperature, pressure, and mechanical tolerance are prerequisites. Multiple other functional attributes such as electrical conductivity, optical transparency, morphing, and self-repair could be necessary along with the structural attributes. To-date, the incorporation of nanofillers in bio-inspired hierarchical design with precisely tailored interfaces has shown promise and there is an enormous opportunity for innovation.[123]

Similarly, bio-inspired composites are a treasure for other fields such as biomedical implants and sensors via grafts and engineering, energy storage via lightweight batteries, global sustainability via ambient processing and self-repair, as well as communication and coding via adaptivity and hidden functionalities. In addition, the ambient assembly processes reveal important lessons to emulate in the broader context of materials recycling and upcycling.

Recent developments of laser-grade bio-inspired photonic bandgap materials also showcase the potential for unprecedented applications beyond structural means such as optical communication and adaptive camouflaging. The insights from bioinspired cross-platform approaches answer practically relevant questions such as the high strength of silk, the emergence of disease, the creation of new materials, and the underpinning philosophy of what constitutes a material. The translation among various hierarchical systems poses a new paradigm for elucidating the fundamental biogenic fabrication processes and emergence of advanced properties in materials. Therefore, a new horizon of engineered living materials can provide unique opportunities to create intelligent materials on demand by combining nature and synthetic analogs for self-organizing, self-sustained, self-powered, and self-evolving structures of synthetic living matter.[124]

Bonded and Nonbonded Interactions

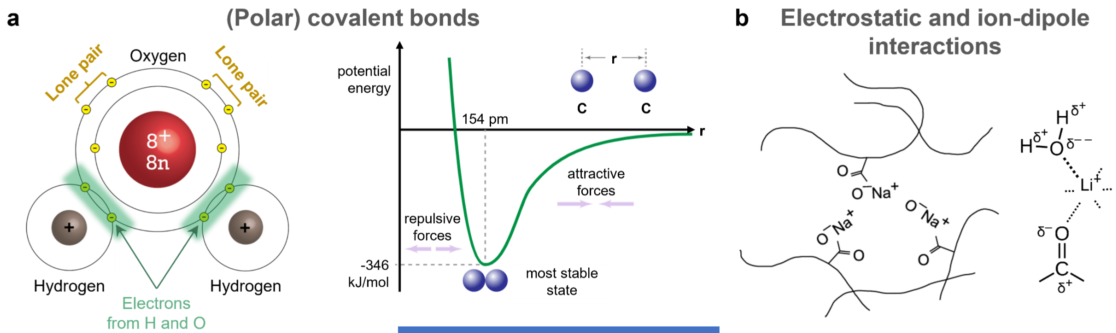

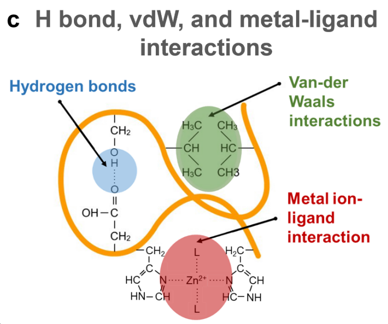

Type of interaction	Equilibrium energy (kJ mol^{-1})
Covalent bond	100 – 900
Electrostatic	100 – 500
Ion-dipole	30 – 200
Hydrogen bond	10 – 65
Cation-π	5 – 80
Metal ion-ligand	0 – 400
π-π	0 – 50
Van-der-Waals	0 – 5
Hydrophobic	Difficult to assess

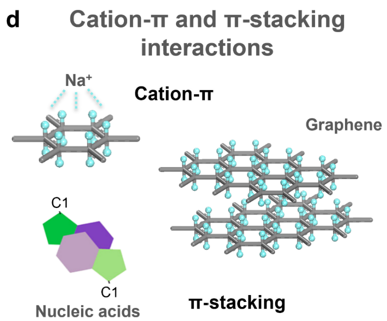

Assembly into Higher Order Structures

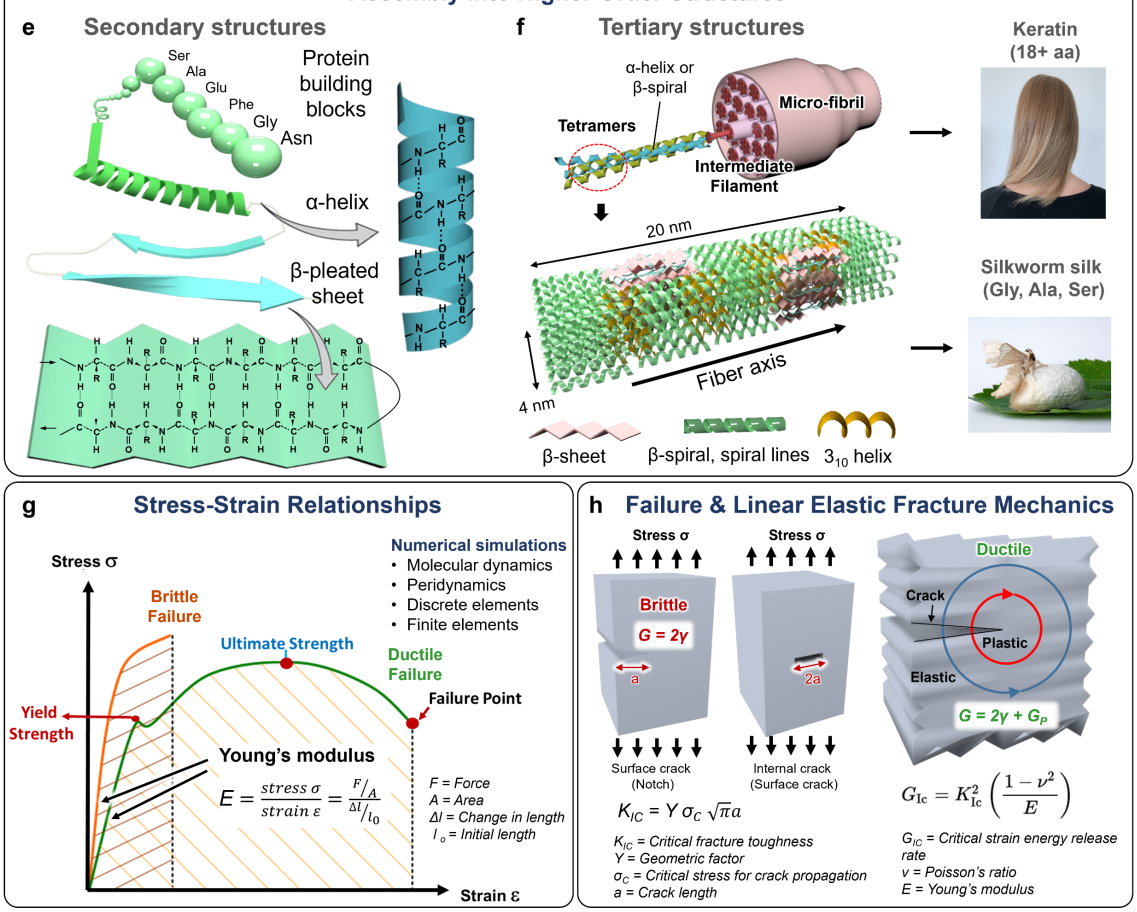

Box 1 | **Fundamentals of interatomic interactions, hierarchical structures, and mechanical behavior.** The primary structure of inorganic and organic compounds is determined by chemical and physical interactions of various strengths (**a-d**).[125] The molecular structure usually involves covalent bonds of varying polarity as shown for water (**a**, left). The potential energy as a function of distance between two atoms resembles a Morse potential, shown for a C-C single bond (**a**, right). Molecular structures are also influenced by non-covalent interactions such as electrostatic interactions (**b**), hydrogen bonds, van-der-Waals forces, metal-ion ligand (**c**), and π-electron related interactions (**d**). Inter- and intramolecular interactions on the weaker end of the energy spectrum are thermally and mechanically reconfigurable and play a major role in generating cohesion via large numbers across material volumes. The full set of bonded and nonbonded interactions, including specific chemistry and solution conditions such as pH value, directs the folding and assembly of larger molecules and building blocks into higher-order structures (**e** and **f**). For example, the sequence of covalently bonded amino acids and the pattern of hydrogen bonds in proteins determines the formation of random coil, α-helix, β-sheet, and other organized building blocks (**e**). These nanometer-scale building blocks can organize into hierarchical structures such as keratin and silk, including α-helical superhelices in keratin and mechanical stabilization of silk fibrils by β-sheet nanocrystals (**f**).[8] Key mechanical properties are derived from stress-strain curves, which are obtained by gradually applying a load (stress) to a test sample and measuring the deformation (strain) (**g**). Fracture mechanics analyzes the propagation of cracks and failure in materials (**h**).[99] Brittle materials fail by crack propagation whereas ductile materials undergo additional plastic deformation, including craze formation in polymers near the crack tip. Crack growth in brittle materials occurs when the increase in surface energy γ of cracks is compensated by a decrease in strain energy via stress release (Griffith theory, total energy for crack growth $G = 2\gamma$). In ductile materials, the total free energy for crack growth is dominated by plastic deformation G_P and follows the more general Irwin theory ($G = 2\gamma + G_P$).

End Box 1

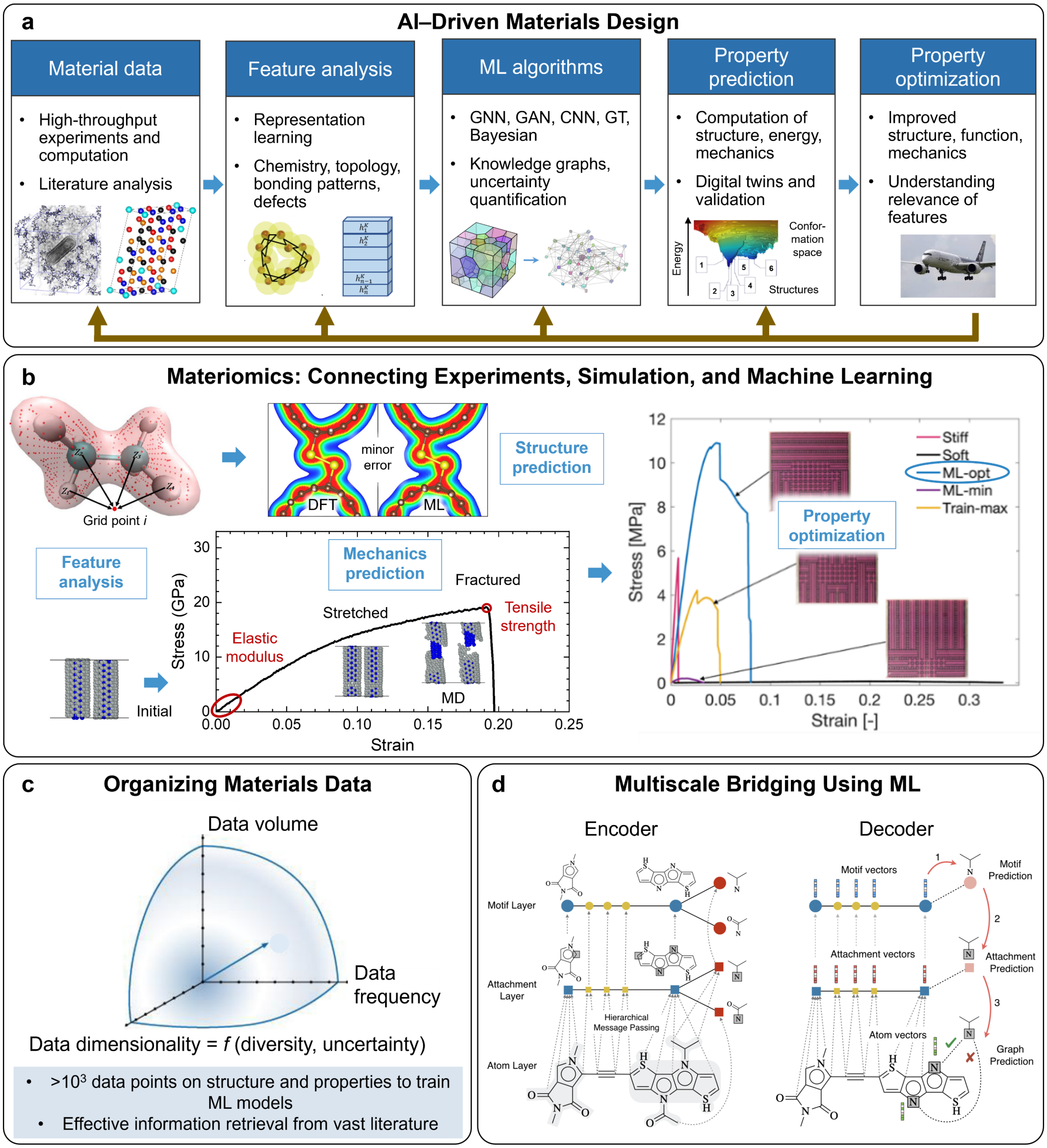

Box 2 | **Tools needed to further advance the field: AI, materiomics, and multi-scale design.** High throughput experimentation and machine learning hold great promise to better sample the vast design space (**a**). Typically, large amounts of data for one type of systems, about thousands to millions, can be categorized into features and vector representations for ML analysis. Examples of data sources include high volumes of X-ray scattering and spectroscopy data, stacks of images from microscopy and tomography, as well as data from computational structure-property calculations. Thereby, the structural and other physical data elements need to be supplied together with the corresponding physical properties of interest for prediction in the entire dataset, i.e., in computer science language, all structural "data" require "labels", to be able to build and train an ML algorithm. The algorithm, once trained, can be applied to predict structural, energetic, mechanical, electronic, and other properties for new material structures within and outside the training space. The integration of cutting-edge experimental data into cross-scale simulations and machine learning facilitates a build-measure-learn feedback loop to construct interpretable digital platforms (digital twins) for faster property optimization. As an example, ML of electronic density features from DFT can be used to predict the atomic-scale structure (**b)**. ML of data from MD simulations can predict stress-strain curves for carbon composites with known defects, allowing recommendation of new designs with increased toughness in a feedback loop with experimental data.[115] The ever-increasing amount of materials data requires tools for systematic organization, considering data volume, frequency of data generation, dimensionality, and uncertainties (**c**). Typically, at least thousands of data points are needed to train effective ML models. It is often challenging to retrieve validated information including uncertainties from the rapidly growing number of publications. Hierarchical graph encoders and decoders for molecular structures can be used to accomplish reversible dimensionality reduction to when solving multiscale problems by ML (**d**).[122] The approaches have promise to overcome longstanding challenges in multiscale modeling and materials design.

End Box 2

Acknowledgements:

The authors would like to acknowledge support from multiple sources: DN - Air Force Office of Scientific Research (AFSOR) 18RXCOR060 and 22RXCOR014, KD - ONR N00014-18-1-2528, MRB - AFOSR FA8650-19-2-5209, MJB - AFOSR FATE MURI FA9550-15-1-0514, LH - Office of Naval Research Global N62909-18-1-2024, SK - PECASE Award ONR N00014-16-1-3175; GCS - Center for Bio-Inspired Energy Sciences (CBES), an Energy Frontiers Research Center (EFRC) under DE-SC0000989, VT - Air Force Research Laboratory FA8650-16-D-5404, AFOSR FA9550-20-1-0305, and NSF-CBET 180349, LCB - AFOSR FA9550-18-1-0381, JAE NSF Career Award CMMI-1454072, PVC - Engineering and Physical Sciences Research Council, grant number EP/R029598/1, HH - NSF 1940335, NSF 1931587, and NASA Space Technology Research Institute STRI-NNX17AJ32G.

References

1. Wegst, U.G.K., Bai, H., Saiz, E., Tomsia, A.P. & Ritchie, R.O. Bioinspired Structural Materials. *Nat. Mater.* **14**, 23-36 (2015).
2. Liu, Z.Q., Meyers, M.A., Zhang, Z.F. & Ritchie, R.O. Functional Gradients and Heterogeneities in Biological Materials: Design Principles, Functions, and Bioinspired Applications. *Progr. Mater. Sci.* **88**, 467-498 (2017).
3. Clancy, A.J., Anthony, D.B. & De Luca, F. Metal Mimics: Lightweight, Strong, and Tough Nanocomposites and Nanomaterial Assemblies. *ACS Appl. Mater. Interfaces* **12**, 15955-15975 (2020).
4. Ritchie, R.O. The Conflicts Between Strength and Toughness. *Nat. Mater.* **10**, 817-822 (2011).
5. Kotov, N.A., Dekany, I. & Fendler, J.H. Ultrathin Graphite Oxide-Polyelectrolyte Composites Prepared by Self-Assembly: Transition Between Conductive and Non-Conductive States. *Adv. Mater.* **8**, 637-641 (1996).
6. Huang, W. et al. Multiscale Toughening Mechanisms in Biological Materials and Bioinspired Designs. *Adv. Mater.* **31**, 1901561 (2019).
7. Tadepalli, S., Slocik, J.M., Gupta, M.K., Naik, R.R. & Singamaneni, S. Bio-Optics and Bio-Inspired Optical Materials. *Chem. Rev.* **117**, 12705-12763 (2017).
8. Wang, B., Yang, W., McKittrick, J. & Meyers, M.A. Keratin: Structure, Mechanical Properties, Occurrence in Biological Organisms, and Efforts at Bioinspiration. *Progr. Mater. Sci.* **76**, 229-318 (2016).
9. Chen, M.L. et al. The Hierarchical Structure and Mechanical Performance of a Natural Nanocomposite Material: The Turtle Shell. *Coll. Surf. a-Physicochem. Eng. Aspects* **520**, 97-104 (2017).
10. Hieronymus, T.L., Witmer, L.M. & Ridgely, R.C. Structure of White Rhinoceros (Ceratotherium simum) Horn Investigated by X-ray Computed Tomography and Histology With Implications for Growth and External Form. *J. Morphology* **267**, 1172-1176 (2006).
11. Teyssier, J., Saenko, S.V., van der Marel, D. & Milinkovitch, M.C. Photonic Crystals Cause Active Colour Change in Chameleons. *Nat. Commun.* **6**, 6368 (2015).
12. Huang, W. et al. A Natural Energy Absorbent Polymer Composite: The Equine Hoof Wall. *Acta Biomater.* **90**, 267-277 (2019).
13. Chon, M.J. et al. Lamellae Spatial Distribution Modulates Fracture Behavior and Toughness of African Pangolin Scales. *J. Mech. Behav. Biomed. Mater.* **76**, 30-37 (2017).
14. Ren, J. et al. Biological Material Interfaces as Inspiration for Mechanical and Optical Material Designs. *Chem. Rev.* **119**, 12279-12336 (2019).
15. Morits, M. et al. Toughness and Fracture Properties in Nacre-Mimetic Clay/Polymer Nanocomposites. *Adv. Funct. Mater.* **27**, 1605378 (2017).
16. Natarajan, B. & Gilman, J. Bioinspired Bouligand Cellulose Nanocrystal Composites: A Review of Mechanical Properties. *Philos. Trans. A Math. Phys. Eng. Sci.* **376**, 20170050 (2018).
17. Grant, A.M. et al. Silk Fibroin-Substrate Interactions at Heterogeneous Nanocomposite Interfaces. *Adv. Funct. Mater.* **26**, 6380-6392 (2016).
18. Wang, Q. et al. Observations of 3 nm Silk Nanofibrils Exfoliated from Natural Silkworm Silk Fibers. *ACS Mater. Lett.* **2**, 153-160 (2020).

19. Shao, Z.Z. & Vollrath, F. Surprising Strength of Silkworm Silk. *Nature* **418**, 741-741 (2002).
20. Guarin-Zapata, N., Gomez, J., Yaraghi, N., Kisailus, D. & Zavattieri, P.D. Shear Wave Filtering in Naturally-occurring Bouligand Structures. *Acta Biomater.* **23**, 11-20 (2015).
21. Gao, H.L. et al. Mass Production of Bulk Artificial Nacre with Excellent Mechanical Properties. *Nat. Comm.* **8**, 287 (2017).
22. Das, P. et al. Nacre-mimetics with Synthetic Nanoclays up to Ultrahigh Aspect Ratios. *Nat. Commun.* **6**, 5967 (2015).
23. Hu, K., Gupta, M.K., Kulkarni, D.D. & Tsukruk, V.V. Ultra-Robust Graphene Oxide-Silk Fibroin Nanocomposite Membranes. *Adv. Mater.* **25**, 2301-2307 (2013).
24. Adamcik, J. et al. Measurement of Intrinsic Properties of Amyloid Fibrils by the Peak Force QNM Method. *Nanoscale* **4**, 4426-4429 (2012).
25. Feng, W.C. et al. Assembly of Mesoscale Helices with Near-unity Enantiomeric Excess and Light-Matter Interactions for Chiral Semiconductors. *Sci. Adv.* **3**, e1601159 (2017).
26. Adstedt, K. et al. Chiral Cellulose Nanocrystals with Intercalated Amorphous Polysaccharides for Controlled Iridescence and Enhanced Mechanics. *Adv. Funct. Mater.* **30**, 2003597 (2020).
27. Cao, Y.P., Bolisetty, S., Wolfisberg, G., Adamcik, J. & Mezzenga, R. Amyloid Fibril-directed Synthesis of Silica Core-Shell Nanofilaments, Gels, and Aerogels. *Proc. Natl. Acad. Sci. U. S. A.* **116**, 4012-4017 (2019).
28. Mittal, N. et al. Multiscale Control of Nanocellulose Assembly: Transferring Remarkable Nanoscale Fibril Mechanics to Macroscale Fibers. *ACS Nano* **12**, 6378-6388 (2018).
29. Ling, S. et al. Polymorphic Regenerated Silk Fibers Assembled Through Bioinspired Spinning. *Nat. Comm.* **8**, 1387 (2017).
30. Zhao, Q.L., Wang, Y.L., Cui, H.Q. & Du, X.M. Bio-Inspired Sensing and Actuating Materials. *J. Mater. Chem. C* **7**, 6493-6511 (2019).
31. de Espinosa, L.M., Meesorn, W., Moatsou, D. & Weder, C. Bioinspired Polymer Systems with Stimuli-Responsive Mechanical Properties. *Chem. Rev.* **117**, 12851-12892 (2017).
32. Egan, P., Sinko, R., LeDuc, P.R. & Keten, S. The Role of Mechanics in Biological and Bio-Inspired Systems. *Nat. Commun.* **6**, 7418 (2015).
33. Gladman, A.S., Matsumoto, E.A., Nuzzo, R.G., Mahadevan, L. & Lewis, J.A. Biomimetic 4D Printing. *Nat. Mater.* **15**, 413-418 (2016).
34. Ye, C.H. et al. Bimorph Silk Microsheets with Programmable Actuating Behavior: Experimental Analysis and Computer Simulations. *ACS Appl. Mater. Interfaces* **8**, 17694-17706 (2016).
35. Zhang, Y.H. et al. A Mechanically Driven Form of Kirigami as a Route to 3D Mesostructures in Micro/Nanomembranes. *Proc. Natl. Acad. Sci. U. S. A.* **112**, 11757-11764 (2015).
36. Lee, J.H., Lee, J.S., Kim, D.K., Park, C.H. & Lee, H.R. Clinical Outcomes of Silk Patch in Acute Tympanic Membrane Perforation. *Clin. Exp. Otorhinolaryngol.* **8**, 117-122 (2015).

37. Zhao, C. et al. Layered Nanocomposites by Shear-Flow-Induced Alignment of Nanosheets. *Nature* **580**, 210-215 (2020).
38. Podsiadlo, P. et al. Ultrastrong and Stiff Layered Polymer Nanocomposites. *Science* **318**, 80-83 (2007).
39. Bonderer, L.J., Studart, A.R. & Gauckler, L.J. Bioinspired Design and Assembly of Platelet Reinforced Polymer Films. *Science* **319**, 1069-1073 (2008).
40. Grossman, M. et al. Mineral Nano-Interconnectivity Stiffens and Toughens Nacre-Like Composite Materials. *Adv. Mater.* **29**, 1605039 (2017).
41. Bai, H. et al. Bioinspired Hydroxyapatite/Poly(methyl methacrylate) Composite with a Nacre-Mimetic Architecture by a Bidirectional Freezing Method. *Adv. Mater.* **28**, 50-56 (2016).
42. Tan, G.Q. et al. Nature-Inspired Nacre-Like Composites Combining Human Tooth-Matching Elasticity and Hardness with Exceptional Damage Tolerance. *Adv. Mater.* **31**, 1904603 (2019).
43. Mao, L.B. et al. Synthetic Nacre by Predesigned Matrix-Directed Mineralization. *Science* **354**, 107-110 (2016).
44. Tan, Y.P. et al. Infiltration of Chitin by Protein Coacervates Defines the Squid Beak Mechanical Gradient. *Nat. Chem. Biol.* **11**, 488-495 (2015).
45. Gim, J. et al. Nanoscale Deformation Mechanics Reveal Resilience in Nacre of Pinna Nobilis Shell. *Nat. Commun.* **10**, 4822 (2019).
46. Zeng, F.Z. et al. A Bioinspired Ultratough Multifunctional Mica-Based Nanopaper with 3D Aramid Nanofiber Framework as an Electrical Insulating Material. *Acs Nano* **14**, 611-619 (2020).
47. Yin, Z., Hannard, F. & Barthelat, F. Impact-Resistant Nacre-Like Transparent Materials. *Science* **364**, 1260-1263 (2019).
48. Weaver, J.C. et al. The Stomatopod Dactyl Club: A Formidable Damage-Tolerant Biological Hammer. *Science* **336**, 1275-1280 (2012).
49. Grunenfelder, L.K. et al. Bio-inspired Impact-Resistant Composites. *Acta Biomater.* **10**, 3997-4008 (2014).
50. Yang, W. et al. Protective Role of Arapaima Gigas Fish Scales: Structure and Mechanical Behavior. *Acta Biomater.* **10**, 3599-3614 (2014).
51. Huang, W. et al. A Natural Impact-Resistant Bicontinuous Composite Nanoparticle Coating. *Nat. Mater.* **19**, 1236-1243 (2020).
52. Yaraghi, N.A. et al. A Sinusoidally Architected Helicoidal Biocomposite. *Adv. Mater.* **28**, 6835-6844 (2016).
53. Gansel, J.K. et al. Gold Helix Photonic Metamaterial as Broadband Circular Polarizer. *Science* **325**, 1513-1515 (2009).
54. Urban, M.J. et al. Chiral Plasmonic Nanostructures Enabled by Bottom-Up Approaches. in *Ann. Rev. Phys. Chem.*, Vol. 70 (eds. Johnson, M.A. & Martinez, T.J.) 275-299 (2019).
55. Ling, S.J., Kaplan, D.L. & Buehler, M.J. Nanofibrils in Nature and Materials Engineering. *Nat. Rev. Mater.* **3**, 18016 (2018).
56. Nikolov, S. et al. Revealing the Design Principles of High-Performance Biological Composites Using Ab initio and Multiscale Simulations: The Example of Lobster Cuticle. *Adv. Mater.* **22**, 519-526 (2010).

57. Cherpak, V. et al. Robust Chiral Organization of Cellulose Nanocrystals in Capillary Confinement. *Nano Lett.* **18**, 6770-6777 (2018).
58. Guo, J.Q. et al. Biodegradable Laser Arrays Self-Assembled from Plant Resources. *Adv. Mater.* **32**, 2002332 (2020).
59. Lin, Y.S., Wei, C.T., Olevsky, E.A. & Meyers, M.A. Mechanical Properties and the Laminate Structure of Arapaima Gigas Scales. *J. Mech. Behavior Biomed. Mater.* **4**, 1145-1156 (2011).
60. Yazawa, K., Malay, A.D., Masunaga, H., Norma-Rashid, Y. & Numata, K. Simultaneous Effect of Strain Rate and Humidity on the Structure and Mechanical Behavior of Spider Silk. *Comm. Mater.* **1**, 10 (2020).
61. Fu, C.J. et al. Cryogenic Toughness of Natural Silk and a Proposed Structure-Function Relationship. *Mater. Chem. Frontiers* **3**, 2507-2513 (2019).
62. Tung, S.O., Ho, S., Yang, M., Zhang, R.L. & Kotov, N.A. A Dendrite-Suppressing Composite Ion Conductor from Aramid Nanofibres. *Nat. Commun.* **6**, 6152 (2015).
63. Gupta, N., Alred, J.M., Penev, E.S. & Yakobson, B.I. Universal Strength Scaling in Carbon Nanotube Bundles with Frictional Load Transfer. *ACS Nano* **15**, 1342-1350 (2021).
64. Guo, C.C. et al. Thermoplastic Moulding of Regenerated Silk. *Nat. Mater.* **19**, 102-108 (2020).
65. Jolowsky, C., Sweat, R., Park, J.G., Hao, A. & Liang, R. Microstructure Evolution and Self-Assembling of CNT Networks During Mechanical Stretching and Mechanical Properties of Highly Aligned CNT Composites. *Compos. Sci. Tech.* **166**, 125-130 (2018).
66. Pramanik, C., Gissinger, J.R., Kumar, S. & Heinz, H. Carbon Nanotube Dispersion in Solvents and Polymer Solutions: Mechanisms, Assembly, and Preferences. *ACS Nano* **11**, 12805-12816 (2017).
67. Davijani, A.A.B. & Kumar, S. Ordered Wrapping of Poly(methyl methacrylate) on Single Wall Carbon Nanotubes. *Polymer* **70**, 278-281 (2015).
68. Eyckens, D.J. et al. Fiber with Butterfly Wings: Creating Colored Carbon Fibers with Increased Strength, Adhesion, and Reversible Malleability. *ACS Appl. Mater. Interfaces* **11**, 41617-41625 (2019).
69. Heinz, H. et al. Nanoparticle Decoration with Surfactants: Molecular Interactions, Assembly, and Applications. *Surf. Sci. Rep.* **72**, 1-58 (2017).
70. Huang, Y., Sasano, T., Tsujii, Y. & Ohno, K. Well-Defined Polymer-Brush-Coated Rod-Shaped Particles: Synthesis and Formation of Liquid Crystals. *Macromolecules* **49**, 8430-8439 (2016).
71. Liu, Z., Xu, Z., Hu, X. & Gao, C. Lyotropic Liquid Crystal of Polyacrylonitrile-Grafted Graphene Oxide and Its Assembled Continuous Strong Nacre-Mimetic Fibers. *Macromolecules* **46**, 6931-6941 (2013).
72. Naguib, M. Multifunctional Pure MXene Fiber from Liquid Crystals of Only Water and MXene. *ACS Central Science* **6**, 344-346 (2020).
73. Chang, H., Luo, J., Gulgunje, P.V. & Kumar, S. Structural and Functional Fibers. *Ann. Rev. Mater. Res.* **47**, 13.1-13.29 (2017).
74. Bakhtiary Davijani, A.A., Chang, H., Liu, H.C., Luo, J. & Kumar, S. Stress Transfer in Nanocomposites Enabled by Poly(methyl methacrylate) Wrapping of Carbon Nanotubes. *Polymer* **130**, 191-198 (2017).

75. Asai, M., Zhao, D. & Kumar, S.K. Role of Grafting Mechanism on the Polymer Coverage and Self-Assembly of Hairy Nanoparticles. *ACS Nano* **11**, 7028-7035 (2017).
76. Hansoge, N.K. et al. Materials by Design for Stiff and Tough Hairy Nanoparticle Assemblies. *ACS Nano* **12**, 7946-7958 (2018).
77. Xu, H. et al. Obtaining High Mechanical Performance Silk Fibers by Feeding Purified Carbon Nanotube/Lignosulfonate Composite to Silkworms. *RSC Adv.* **9**, 3558-3569 (2019).
78. Jiang, C. et al. Mechanical Properties of Robust Ultrathin Silk Fibroin Films. *Adv. Funct. Mater.* **17**, 2229-2237 (2007).
79. Podsiadlo, P., Tang, Z., Shim, B.S. & Kotov, N.A. Counterintuitive Effect of Molecular Strength and Role of Molecular Rigidity on Mechanical Properties of Layer-by-Layer Assembled Nanocomposites. *Nano Lett.* **7**, 1224-1231 (2007).
80. Svagan, A.J., Samir, M.A.S.A. & Berglund, L.A. Biomimetic Foams of High Mechanical Performance Based on Nanostructured Cell Walls Reinforced by Native Cellulose Nanofibrils. *Adv. Mater.* **20**, 1263-1269 (2008).
81. Xiong, R. et al. Ultrarobust Transparent Cellulose Nanocrystal-Graphene Membranes with High Electrical Conductivity. *Adv. Mater.* **28**, 1501-1509 (2016).
82. Munch, E. et al. Tough, Bio-Inspired Hybrid Materials. *Science* **322**, 1516-1520 (2008).
83. Djumas, L., Molotnikov, A., Simon, G.P. & Estrin, Y. Enhanced Mechanical Performance of Bio-Inspired Hybrid Structures Utilising Topological Interlocking Geometry. *Sci. Rep.* **6**, 26706 (2016).
84. Cheng, Q., Jiang, L. & Tang, Z. Bioinspired Layered Materials with Superior Mechanical Performance. *Acc. Chem. Res.* **47**, 1256-1266 (2014).
85. Zhang, Y. et al. Bioinspired, Graphene-enabled Ni Composites with High Strength and Toughness. *Sci. Adv.* **5**, eaav5577 (2019).
86. Raut, H.K. et al. Tough and Strong: Cross-Lamella Design Imparts Multifunctionality to Biomimetic Nacre. *ACS Nano* **14**, 9771-9779 (2020).
87. Sachs, C., Fabritius, H. & Raabe, D. Influence of Microstructure on Deformation Anisotropy of Mineralized Cuticle from the Lobster Homarus Americanus. *J. Struct. Biol.* **161**, 120-132 (2008).
88. Gu, M., Jiang, C., Liu, D., Prempeh, N. & Smalyukh, I.I. Cellulose Nanocrystal/Poly(ethylene glycol) Composite as an Iridescent Coating on Polymer Substrates: Structure-Color and Interface Adhesion. *ACS Appl. Mater. Interfaces* **8**, 32565-32573 (2016).
89. Wang, B. & Walther, A. Self-Assembled, Iridescent, Crustacean-Mimetic Nanocomposites with Tailored Periodicity and Layered Cuticular Structure. *ACS Nano* **9**, 10637-10646 (2015).
90. Vollick, B., Kuo, P.Y., Therien-Aubin, H., Yan, N. & Kumacheva, E. Composite Cholesteric Nanocellulose Films with Enhanced Mechanical Properties. *Chem. Mater.* **29**, 789-795 (2017).
91. Chen, P.-Y., Lin, A.Y.-M., McKittrick, J. & Meyers, M.A. Structure and Mechanical Properties of Crab Exoskeletons. *Acta Biomater.* **4**, 587-596 (2008).
92. Ayutsede, J. et al. Carbon Nanotube Reinforced Bombyx mori Silk Nanofibers by the Electrospinning Process. *Biomacromolecules* **7**, 208-214 (2006).

93. Yang, J., Han, C.-R., Zhang, X.-M., Xu, F. & Sun, R.-C. Cellulose Nanocrystals Mechanical Reinforcement in Composite Hydrogels with Multiple Cross-Links: Correlations between Dissipation Properties and Deformation Mechanisms. *Macromolecules* **47**, 4077-4086 (2014).
94. Watanabe, K. et al. Highly Transparent and Tough Filler Composite Elastomer Inspired by the Cornea. *ACS Mater. Lett.* **2**, 325-330 (2020).
95. Pan, H. et al. Significantly Reinforced Composite Fibers Electrospun from Silk Fibroin/Carbon Nanotube Aqueous Solutions. *Biomacromolecules* **13**, 2859-2867 (2012).
96. Wang, J., Cheng, Q., Lin, L. & Jiang, L. Synergistic Toughening of Bioinspired Poly(vinyl alcohol)–Clay–Nanofibrillar Cellulose Artificial Nacre. *ACS Nano* **8**, 2739-2745 (2014).
97. Lönnberg, H., Larsson, K., Lindström, T., Hult, A. & Malmström, E. Synthesis of Polycaprolactone-Grafted Microfibrillated Cellulose for Use in Novel Bionanocomposites–Influence of the Graft Length on the Mechanical Properties. *ACS Appl. Mater. Interfaces* **3**, 1426-1433 (2011).
98. Scaffaro, R. & Maio, A. Integrated Ternary Bionanocomposites with Superior Mechanical Performance via the Synergistic Role of Graphene and Plasma Treated Carbon Nanotubes. *Composites, Part B* **168**, 550-559 (2019).
99. Ashby, M.F. Overview No. 80: On the Engineering Properties of Materials. *Acta Metallurgica* **37**, 1273-1293 (1989).
100. *CES EduPack Software*, (Granta Design Limited, Cambridge, UK, 2009).
101. Dalton, A.B. et al. Super-Tough Carbon-Nanotube Fibres - These Extraordinary Composite Fibres Can Be Woven into Electronic Textiles. *Nature* **423**, 703-703 (2003).
102. Praprotnik, M., Site, L.D. & Kremer, K. Multiscale Simulation of Soft Matter: From Scale Bridging to Adaptive Resolution. *Annu. Rev. Phys. Chem.* **59**, 545-571 (2008).
103. Heinz, H. & Ramezani-Dakhel, H. Simulations of Inorganic–Bioorganic Interfaces to Discover New Materials: Insights, Comparisons to Experiment, Challenges, and Opportunities. *Chem. Soc. Rev.* **45**, 412-448 (2016).
104. Lu, J.X., Luo, M. & Yakobson, B.I. Glass Composites Reinforced with Silicon-Doped Carbon Nanotubes. *Carbon* **128**, 231-236 (2018).
105. Tsafack, T. et al. Exploring the Interface between Single-walled Carbon Nanotubes and Epoxy Resin. *Carbon* **105**, 600-606 (2016).
106. Heinz, H., Lin, T.-J., Mishra, R.K. & Emami, F.S. Thermodynamically Consistent Force Fields for the Assembly of Inorganic, Organic, and Biological Nanostructures: The INTERFACE Force Field. *Langmuir* **29**, 1754-1765 (2013).
107. Mason, J.A. et al. Contraction and Expansion of Stimuli-Responsive DNA Bonds in Flexible Colloidal Crystals. *J. Am. Chem. Soc.* **138**, 8722-8725 (2016).
108. Samanta, D. et al. Multivalent Cation-Induced Actuation of DNA-Mediated Colloidal Superlattices. *J. Am. Chem. Soc.* **141**, 19973-19977 (2019).
109. Gissinger, J.R., Pramanik, C., Newcomb, B., Kumar, S. & Heinz, H. Nanoscale Structure-Property Relationships of Polyacrylonitrile/CNT Composites as a Function of Polymer Crystallinity and CNT Diameter. *ACS Appl. Mater. Interfaces* **10**, 1017-1027 (2018).

110. Zhao, H. et al. NanoMine Schema: An Extensible Data Representation for Polymer Nanocomposites. *APL Materials* **6**, 111108 (2018).
111. Gooneie, A., Schuschnigg, S. & Holzer, C. A Review of Multiscale Computational Methods in Polymeric Materials. *Polymers* **9**, 16 (2017).
112. Ha, Y. & Bobaru, F. Studies of Dynamic Crack Propagation and Crack Branching with Peridynamics. *Int. J. Fracture* **162**, 229-244 (2010).
113. Vassaux, M., Sinclair, R.C., Richardson, R.A., Suter, J.L. & Coveney, P.V. The Role of Graphene in Enhancing the Material Properties of Thermosetting Polymers. *Adv. Theory Simul.* **2**, 1800168 (2019).
114. Guarin-Zapata, N., Gomez, J., Kisailus, D. & Zavattieri, P.D. Bandgap Tuning in Bioinspired Helicoidal Composites. *J. Mech. Phys. Solids* **131**, 344-357 (2019).
115. Gu, G.X., Chen, C.T., Richmond, D.J. & Buehler, M.J. Bioinspired Hierarchical Composite Design Using Machine Learning: Simulation, Additive Manufacturing, and Experiment. *Materials Horizons* **5**, 939-945 (2018).
116. Kronqvist, N. et al. Efficient Protein Production Inspired by How Spiders Make Silk. *Nat. Commun.* **8**, 15504 (2017).
117. Valois, E., Mirshafian, R. & Waite, J.H. Phase-Dependent Redox Insulation in Mussel Adhesion. *Sci. Adv.* **6**, eaaz6486 (2020).
118. Wang, C.Y., Xia, K.L., Zhang, Y.Y. & Kaplan, D.L. Silk-Based Advanced Materials for Soft Electronics. *Acc. Chem. Res.* **52**, 2916-2927 (2019).
119. Wu, Z. et al. A Comprehensive Survey on Graph Neural Networks. *IEEE Transactions on Neural Networks and Learning Systems* **32**, 4-24 (2021).
120. Wang, M.Q. et al. Biomorphic Structural Batteries for Robotics. *Science Robotics* **5**, eaba1912 (2020).
121. Yu, C.H., Qin, Z., Martin-Martinez, F.J. & Buehler, M.J. A Self-Consistent Sonification Method to Translate Amino Acid Sequences into Musical Compositions and Application in Protein Design Using Artificial Intelligence. *ACS Nano* **13**, 7471-7482 (2019).
122. Jin, W., Barzilay, R. & Jaakkola, T. Hierarchical Generation of Molecular Graphs using Structural Motifs. in *Proceedings of the 37th International Conference on Machine Learning* Vol. 119 (eds Hal, D., III & Aarti, S.) 4839-4848 (PMLR, Proceedings of Machine Learning Research, 2020).
123. Lossada, F., Jiao, D., Hoenders, D. & Walther, A. Recyclable and Light-Adaptive Vitrimer-Based Nacre-Mimetic Nanocomposites. *ACS Nano* **15**, 5043-5055 (2021).
124. Xin, A. et al. Growing Living Composites with Ordered Microstructures and Exceptional Mechanical Properties. *Adv. Mater.* **33**, 2006946 (2021).
125. *CRC Handbook of Chemistry and Physics*, (CRC Press, Boca Raton, FL, 2020).